Supplementary Information For:

Synthesis and Characterization of NiAl-Hydride Heterometallics: Perturbing Electron Density Within Al–H–Ni Subunits

Aleida G. Gonzalez[1], Fernando Gonzalez[1], Edgardo De Leon[1], Kaitlyn M. Birkhoff[2], Samantha Yruegas[2], Haoyuan Chen[3,4], and Manar M. Shoshani*[1,5]*

1. School of Integrated Biological and Chemical Sciences, University of Texas Rio Grande Valley, Brownsville Texas, 78520, United States.
2. Department of Chemistry, Rice University, Houston, Texas, 77005, United States.
3. Department of Physics and Astronomy, University of Texas Rio Grande Valley, Edinburg Texas, 78539, United States.
4. Department of Chemistry, Southern Methodist University, Dallas, Texas, 75275, United States
5. Department of Chemistry, University of Kansas, Lawrence, Kansas, 66045, United States

Contents:

S1: NMR spectra of Heterobimetallic Complexes

Figure S1-1: ^{1}H NMR spectrum of **2-(PPh$_3$)$_2$** in C_6D_6

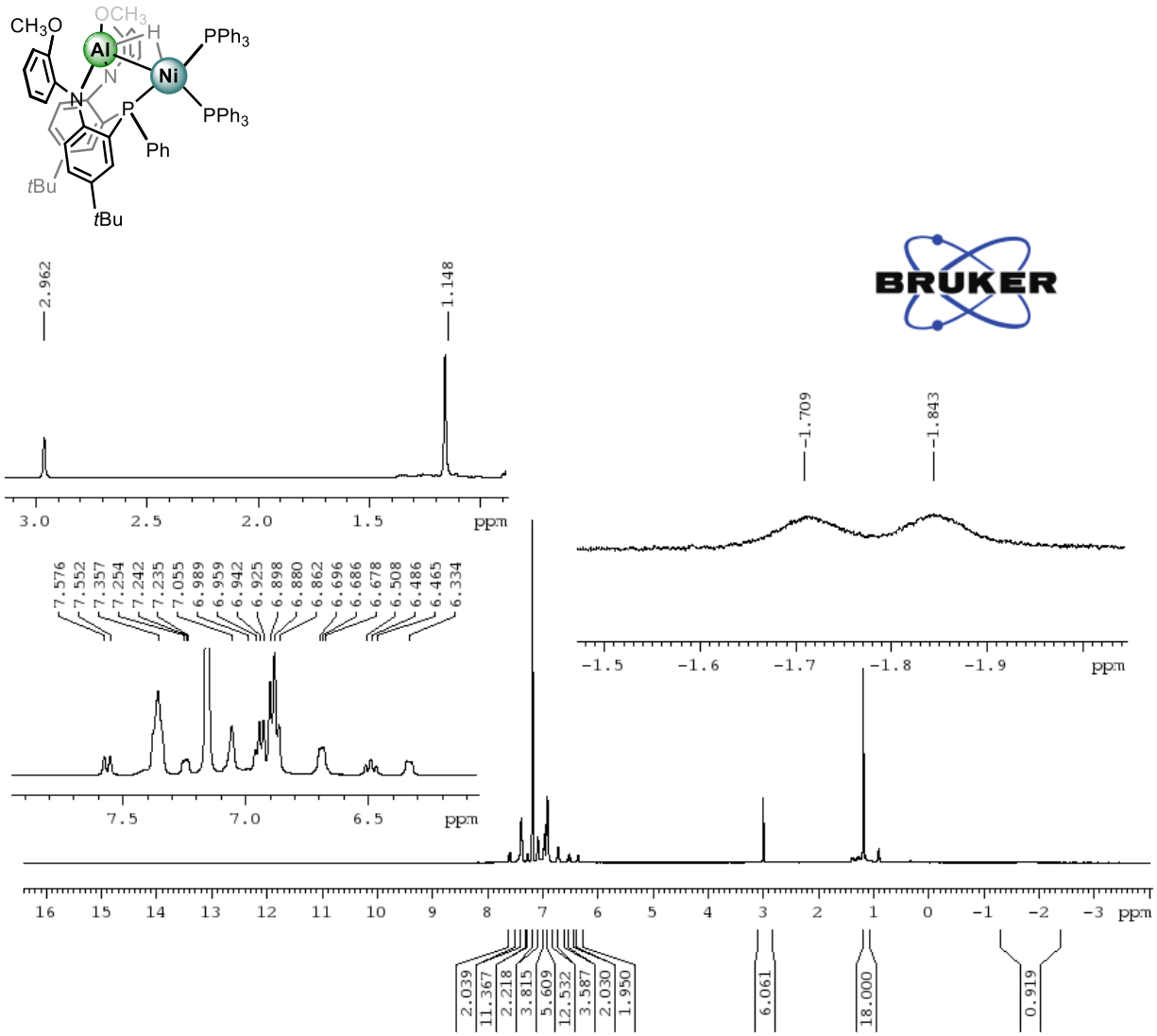

Figure S1-2: $^{31}P\{^{1}H\}$ NMR spectrum of **2-(PPh$_3$)$_2$** in C_6D_6

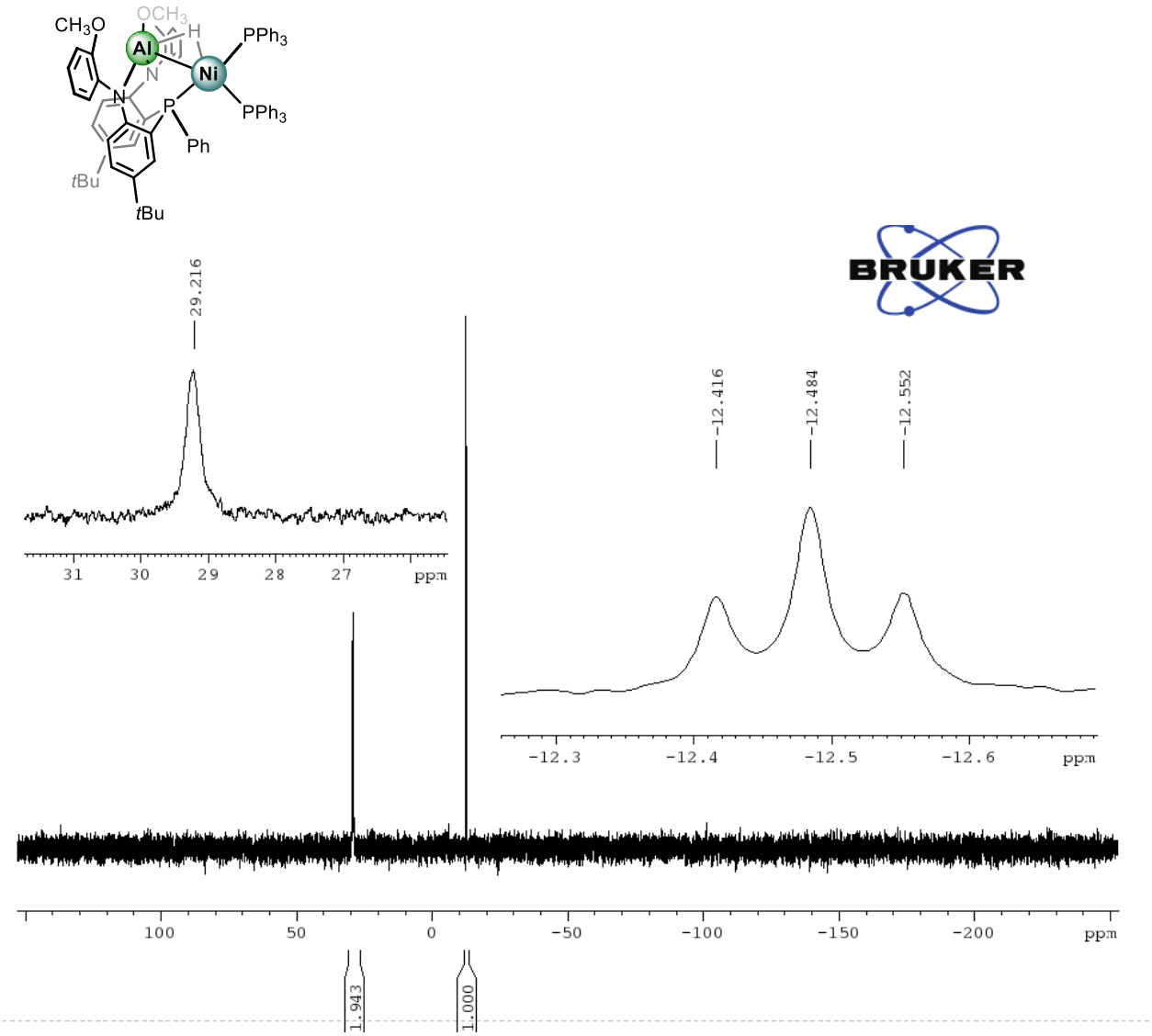

Figure S1-3: $^{13}C\{^{1}H\}$ NMR spectrum of **2-(PPh$_3$)$_2$** in C_6D_6

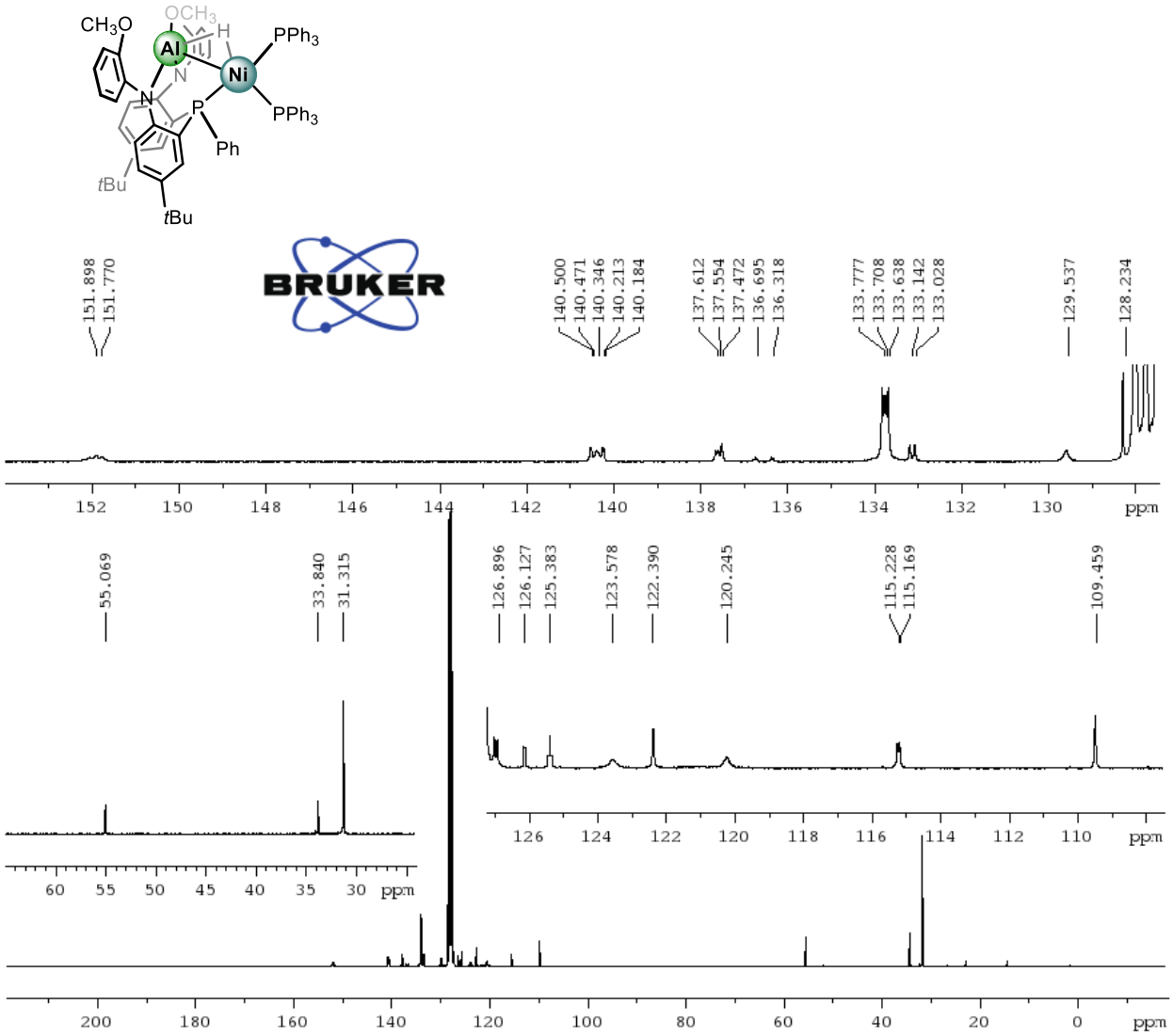

Figure S1-4: ^{1}H NMR spectrum of **2-(dppm)$_2$** in C_6D_6

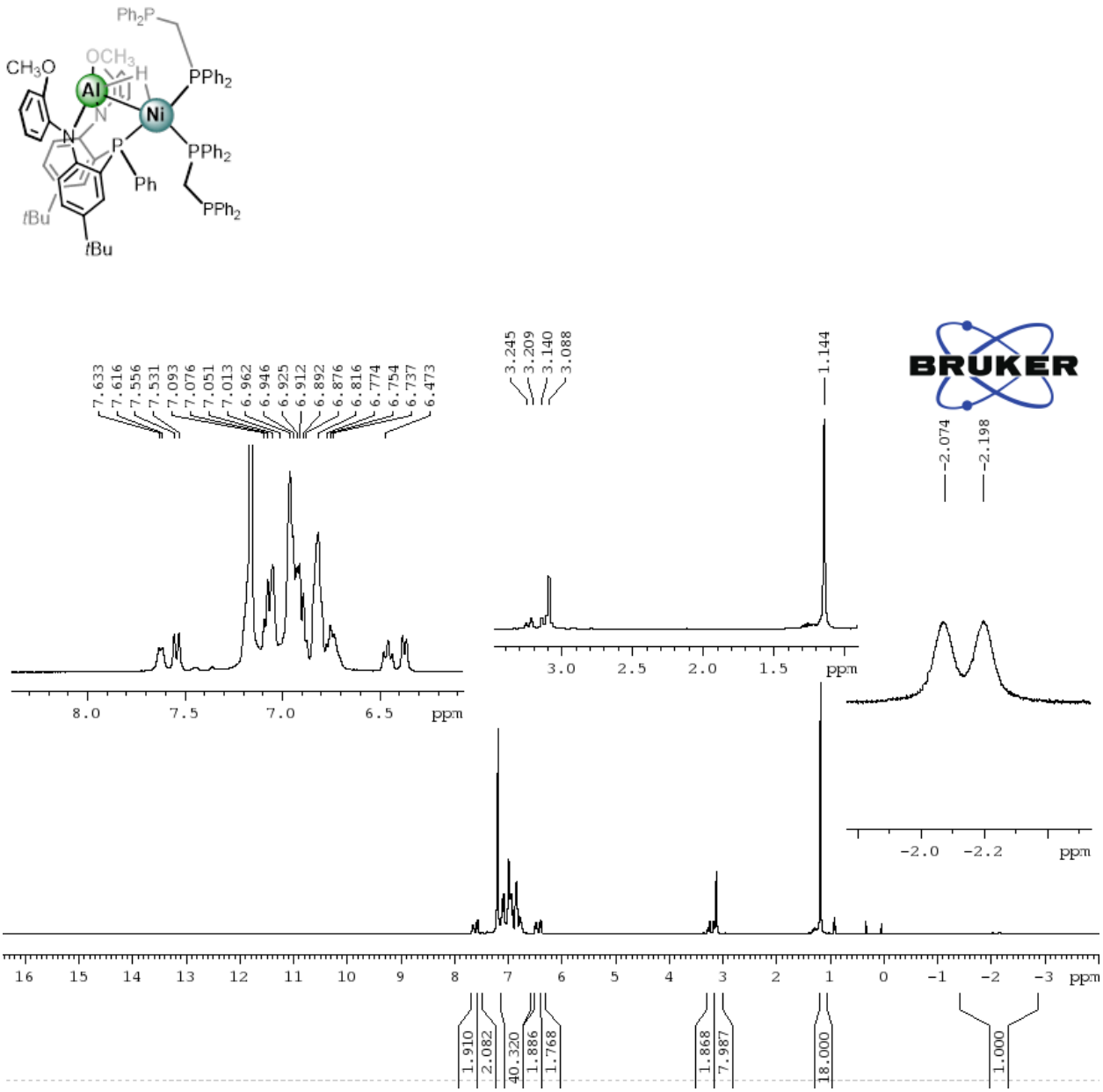

Figure S1-5: $^{31}P\{^{1}H\}$ NMR spectrum of **2-(dppm)$_2$** in C_6D_6

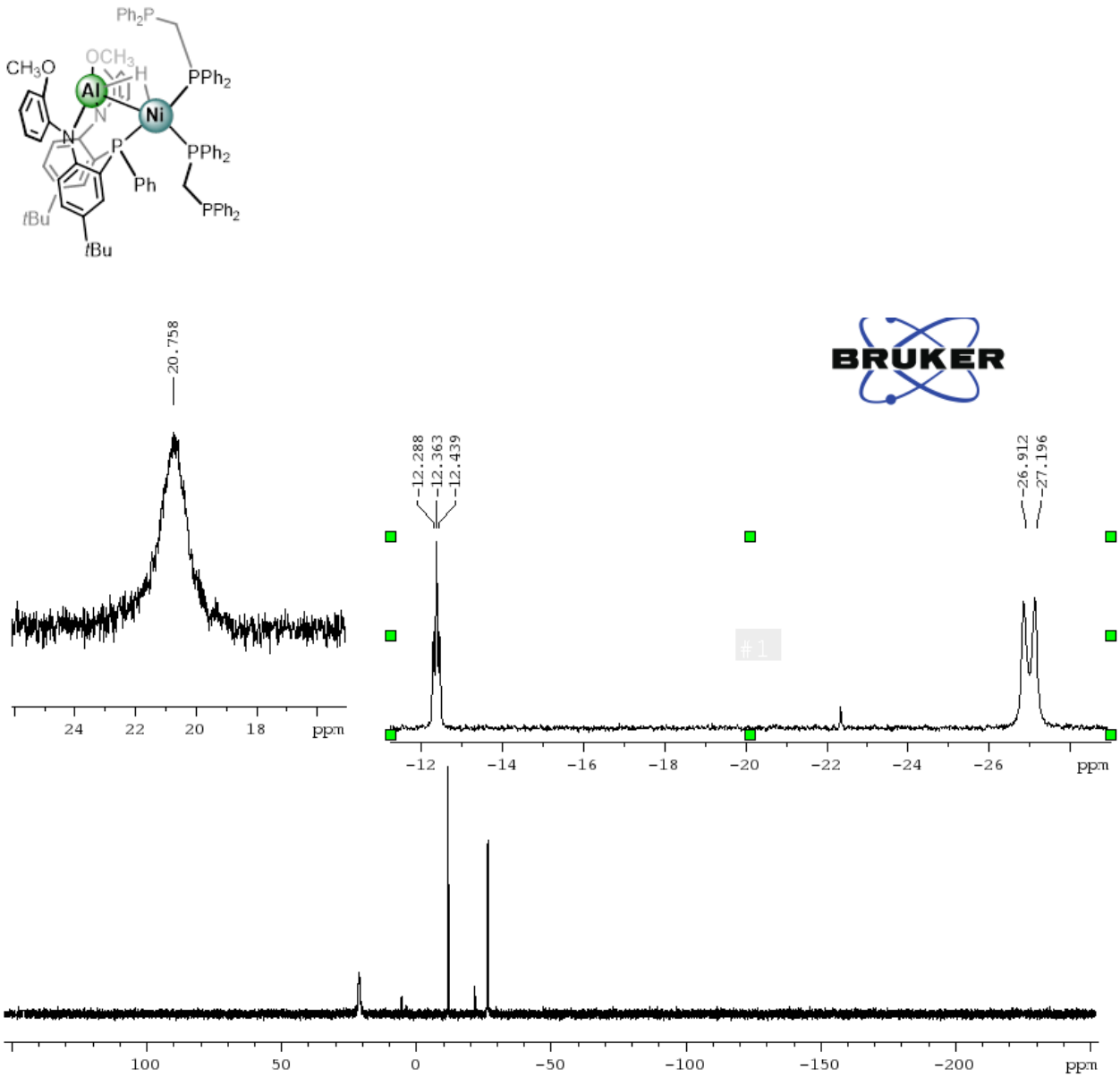

Figure S1-6: $^{13}C\{^{1}H\}$ NMR spectrum of **2-(dppm)$_2$** in C_6D_6

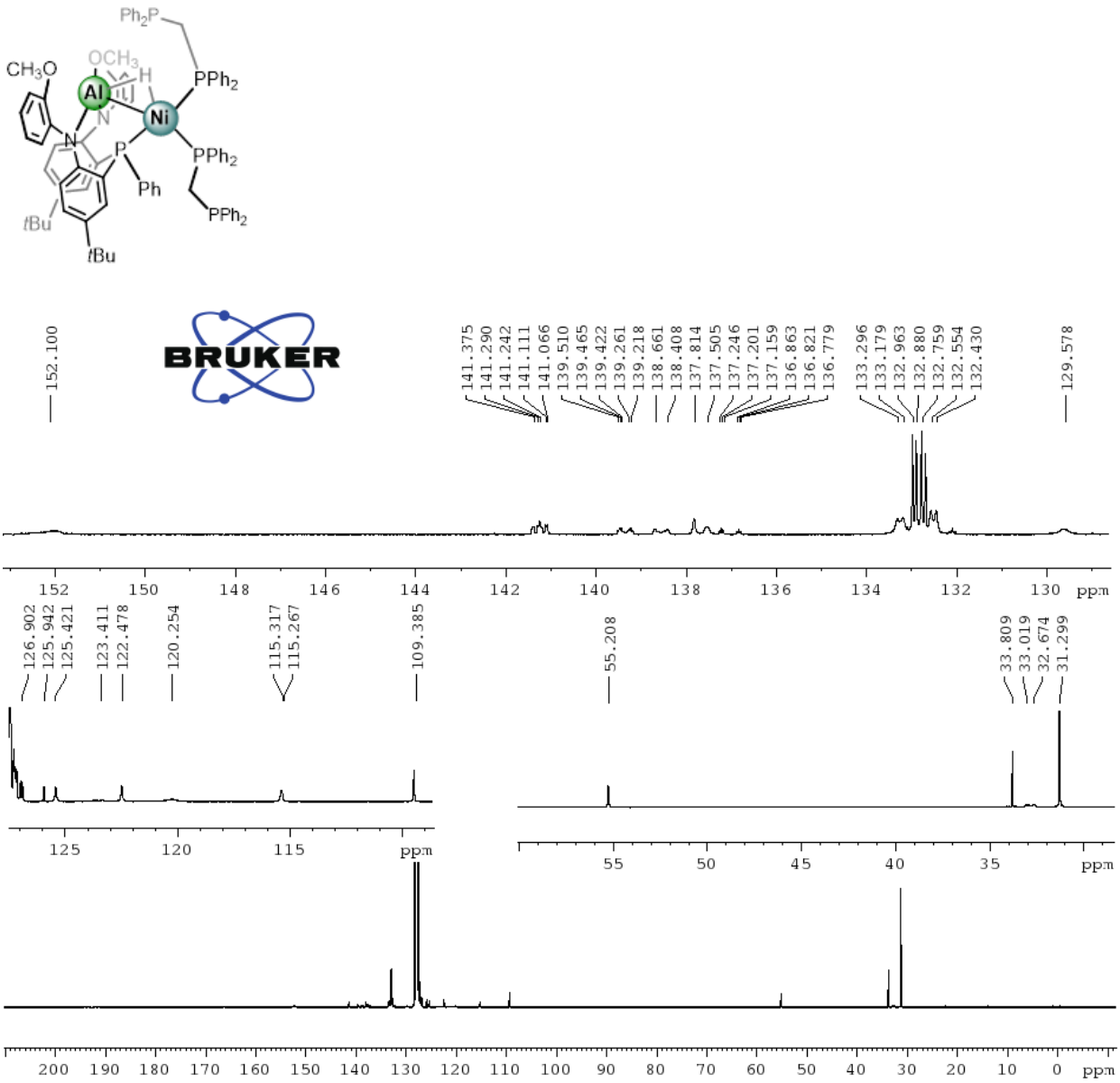

Figure S1-7: ^{1}H NMR spectrum of **2-(PMe$_3$)$_2$** in C_6D_6

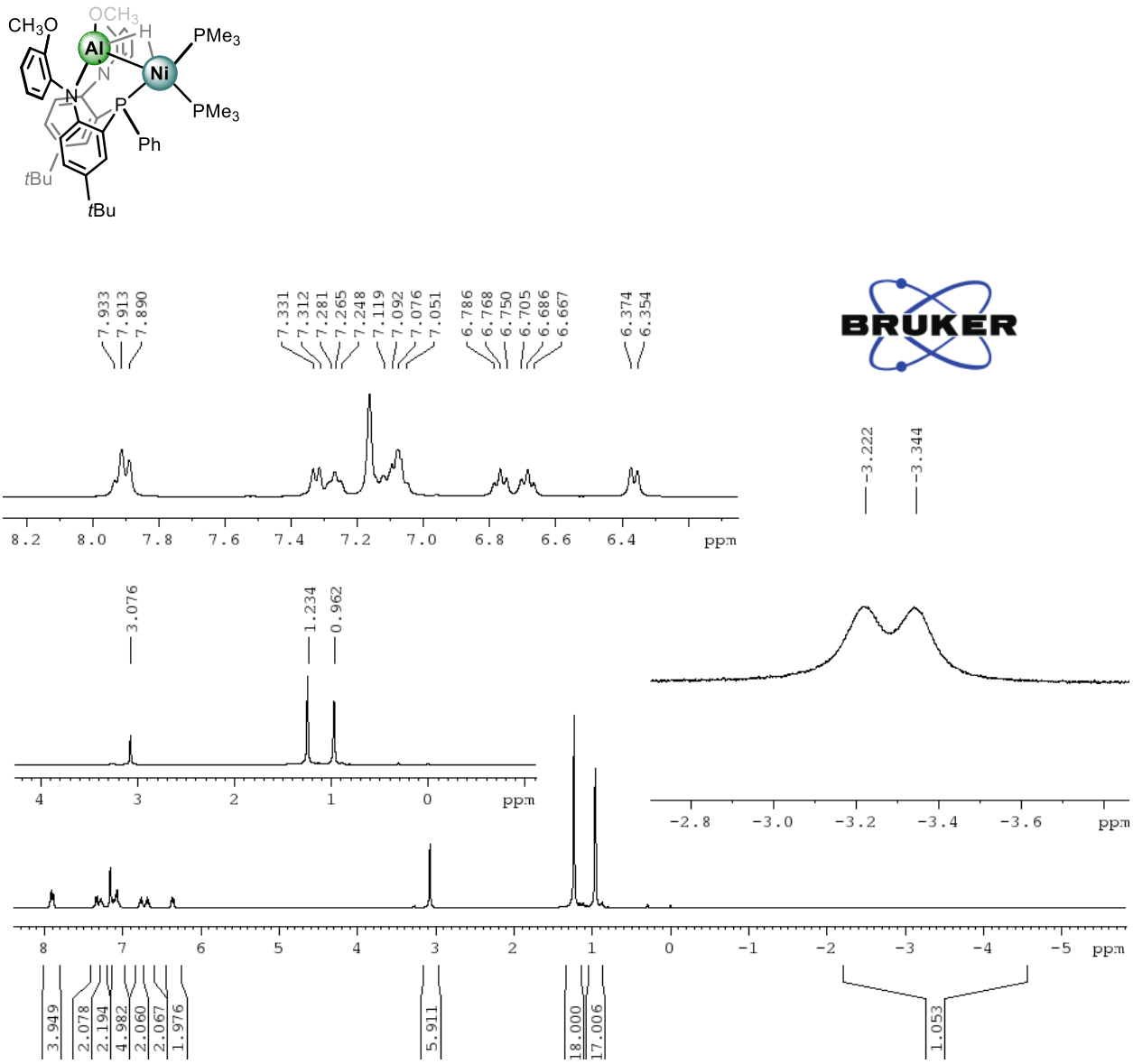

Figure S1-8: $^{31}P\{^{1}H\}$ NMR spectrum of **2-(PMe$_3$)$_2$** in C_6D_6

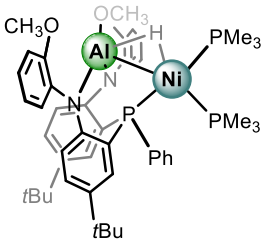

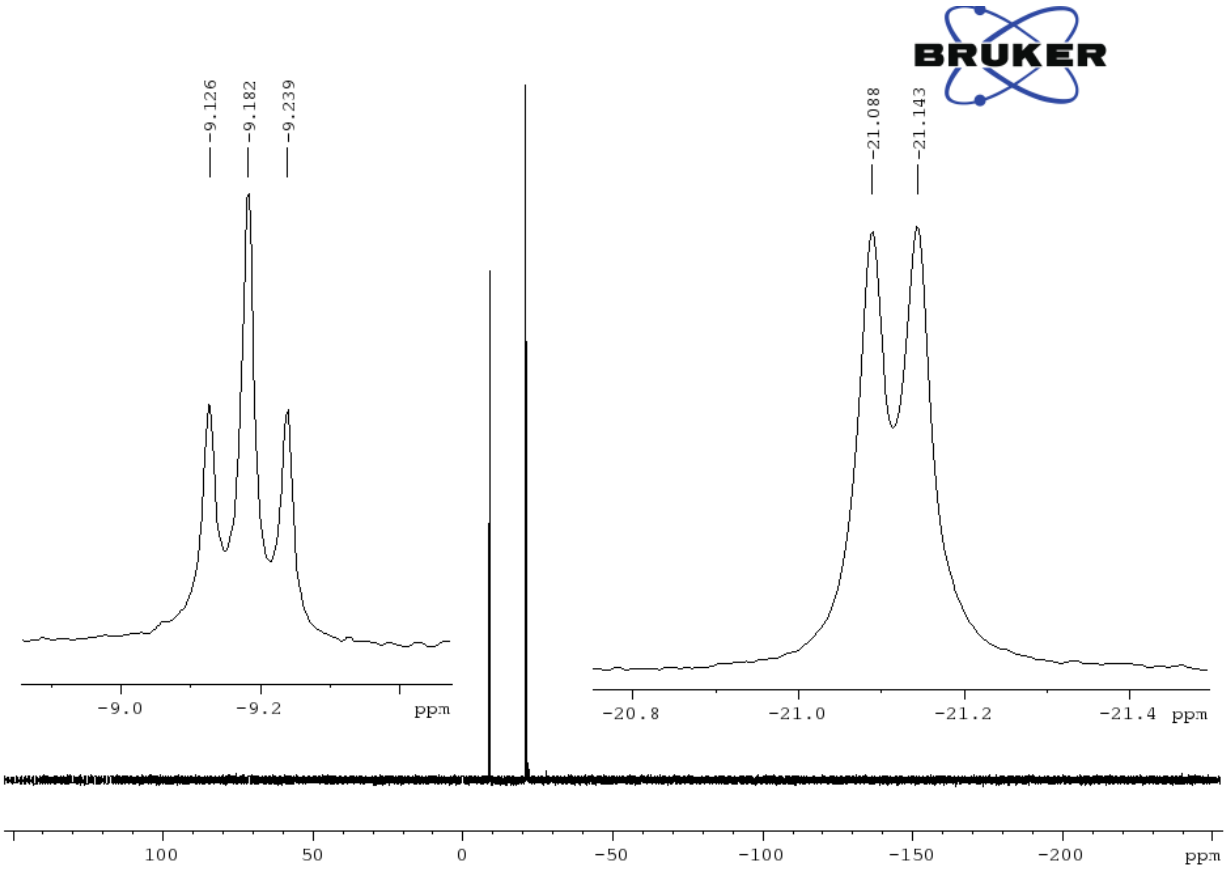

Figure S1-9: $^{13}C\{^{1}H\}$ NMR spectrum of **2-(PMe$_3$)$_2$** in C_6D_6

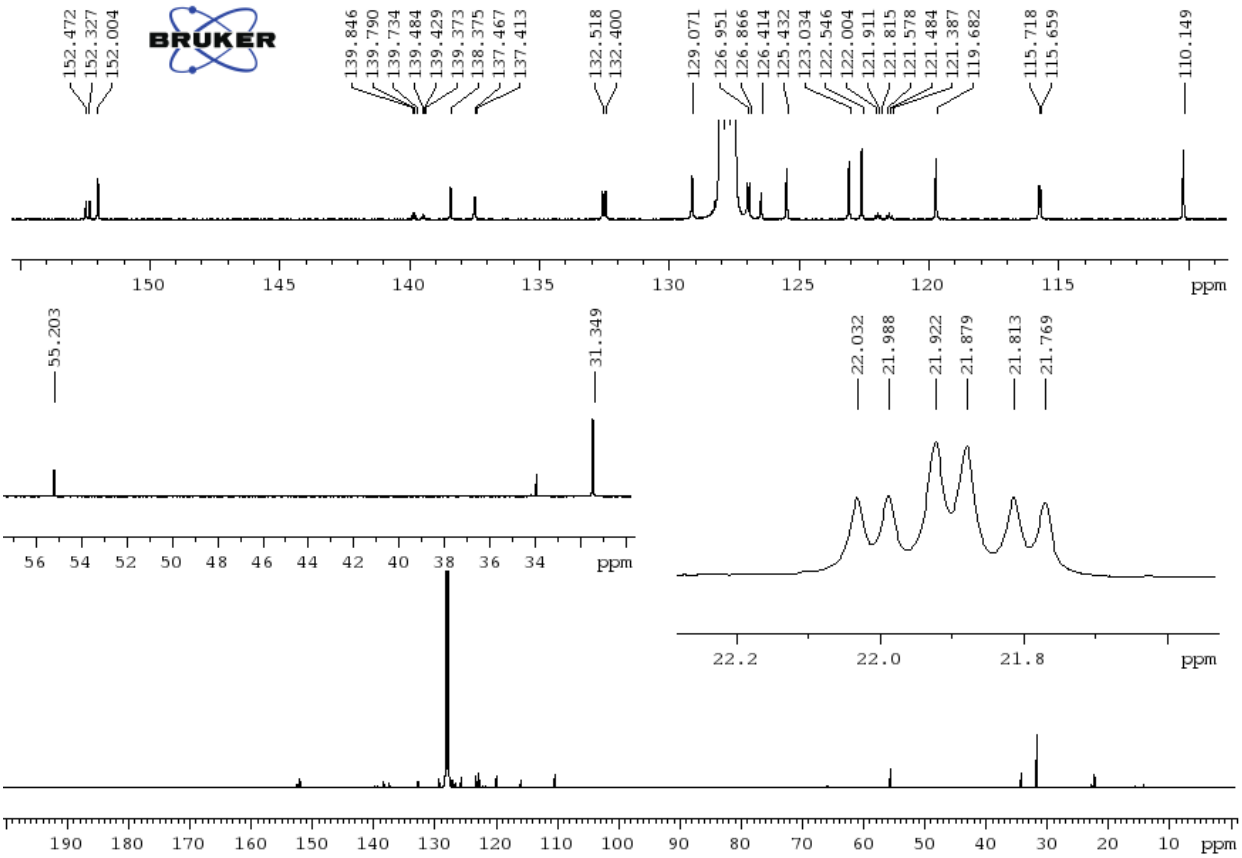

Figure S1-10: ^{1}H NMR spectrum of **3** in THF-D$_8$

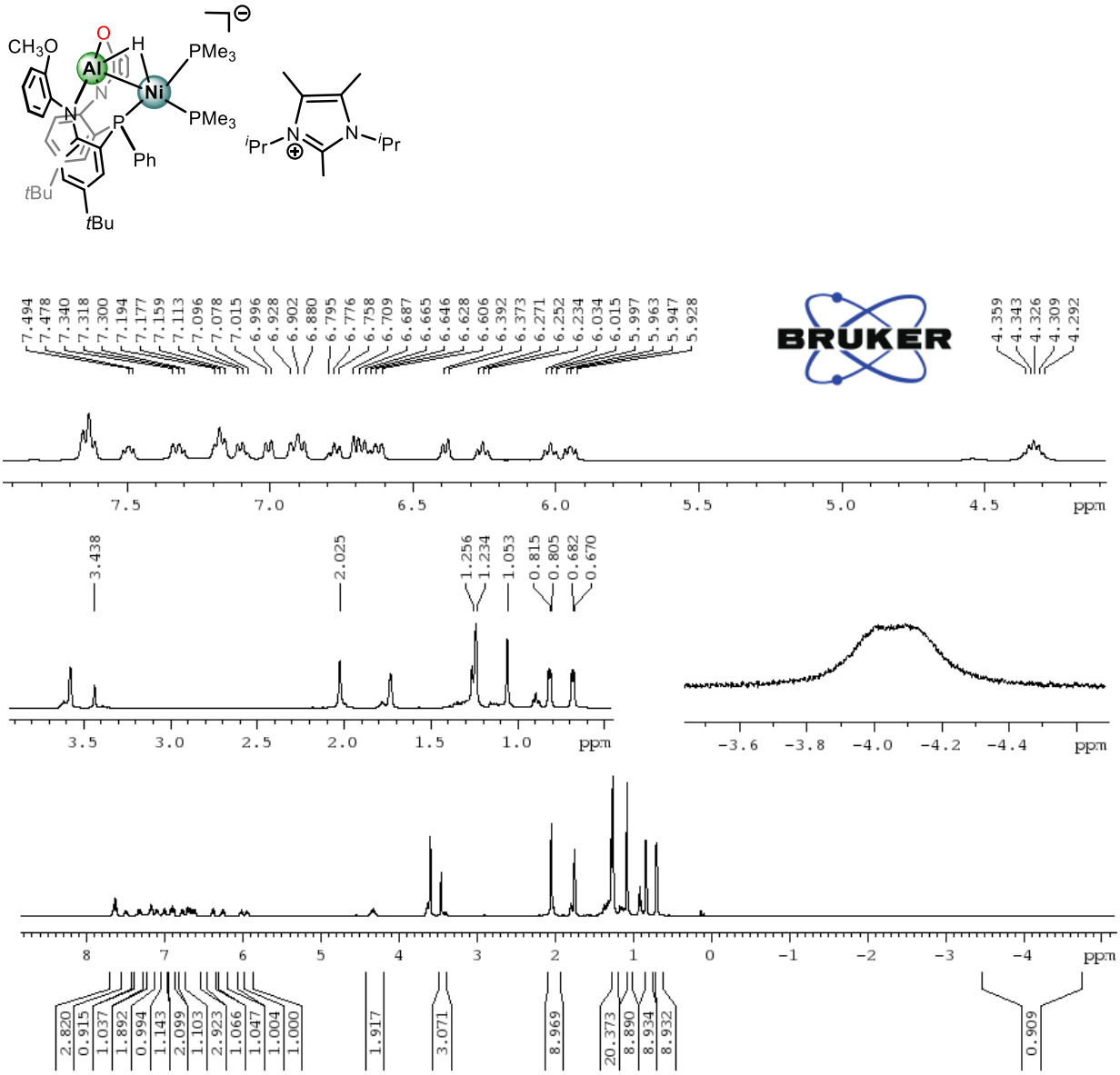

Figure S1-11: $^{31}P\{^{1}H\}$ NMR spectrum of **3** in THF-D_8

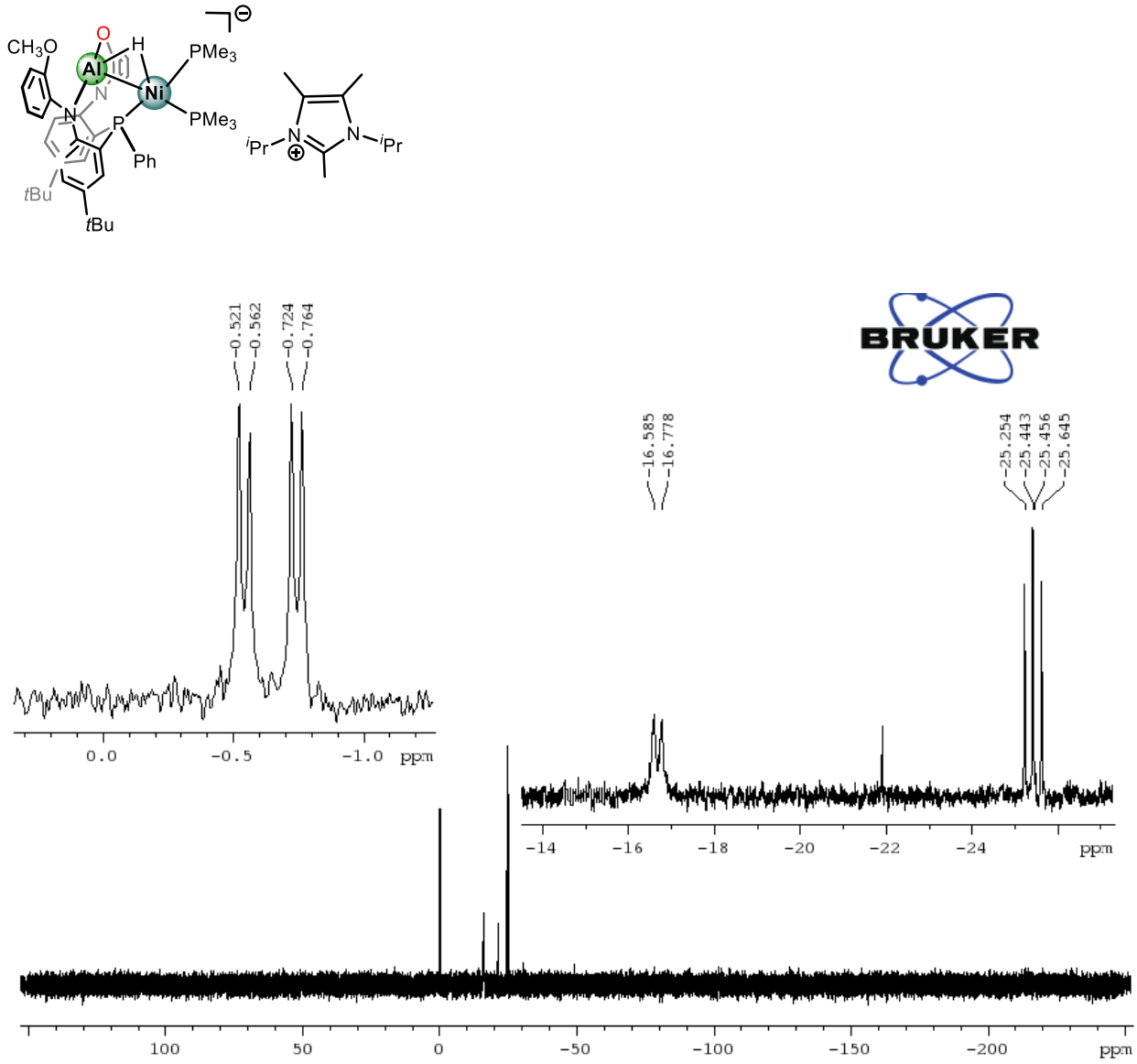

Figure S1-12: APT $^{13}C\{^{1}H\}$ NMR spectrum of **3** in THF-D_8

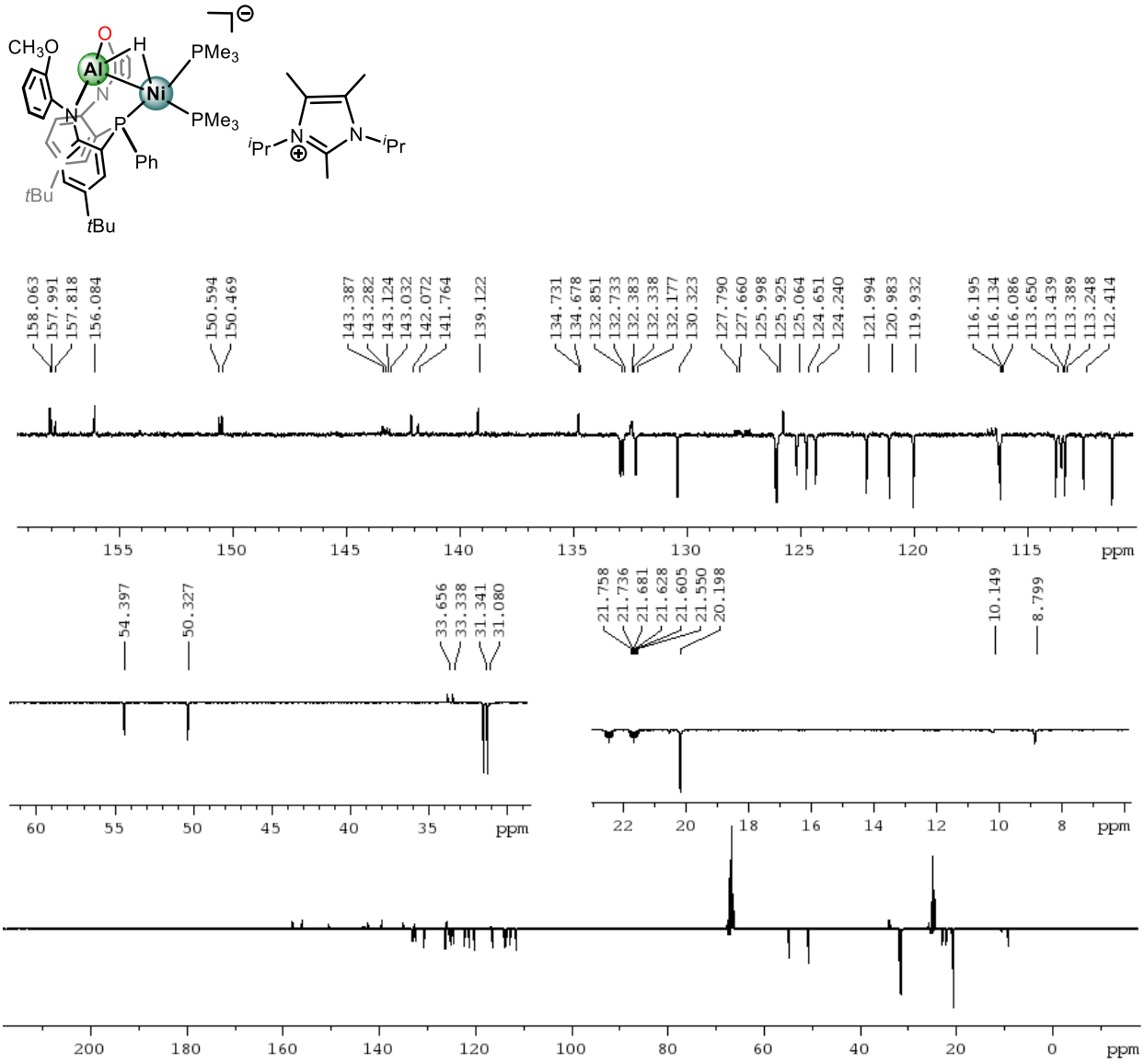

Figure S1-13: $^{1}H^{13}C\{^{1}H\}$ HSQC NMR spectrum of **3** in THF-D_8

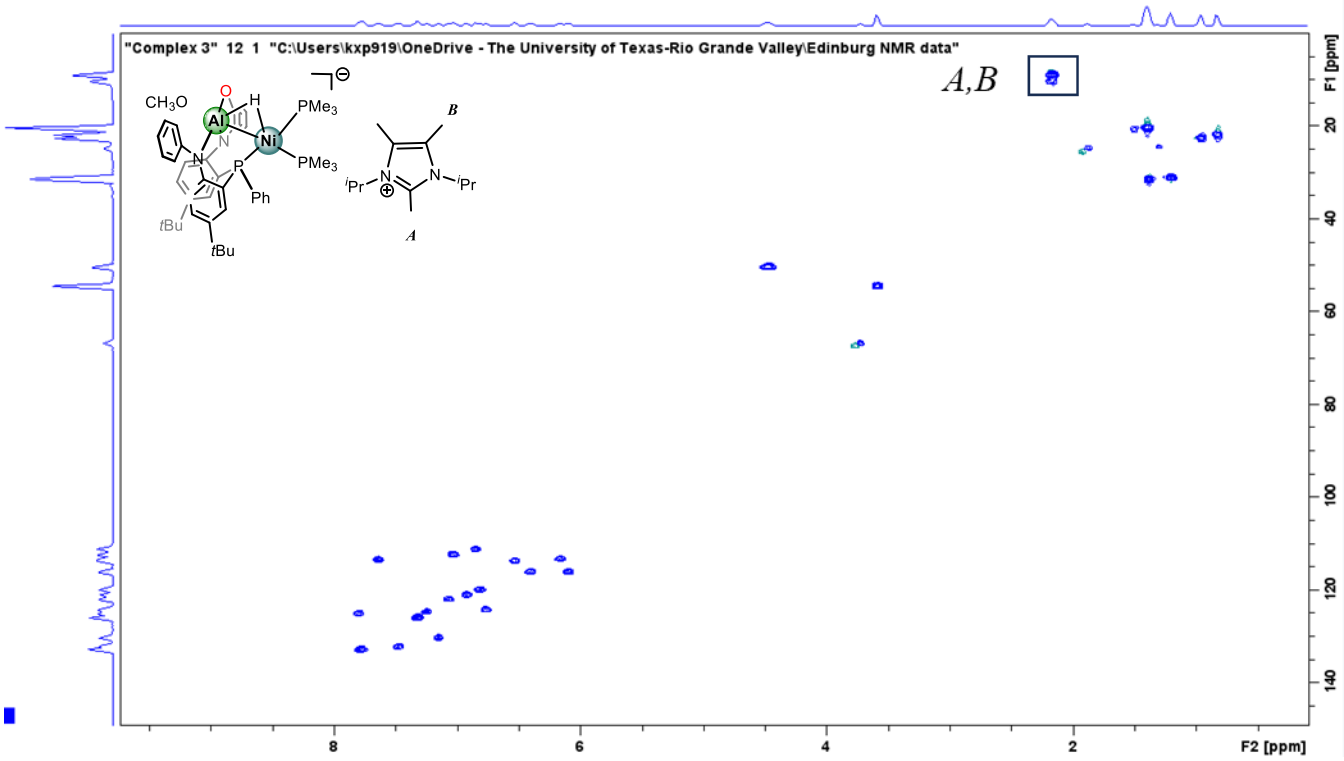

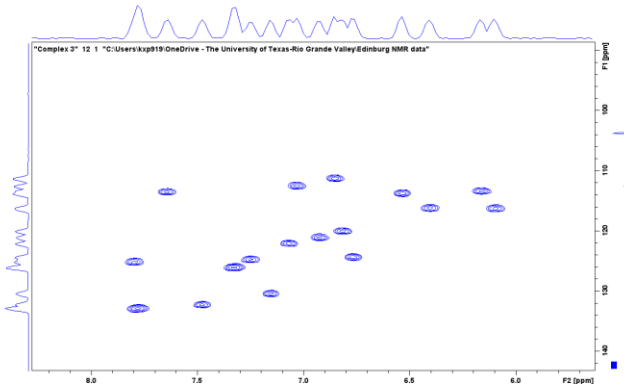

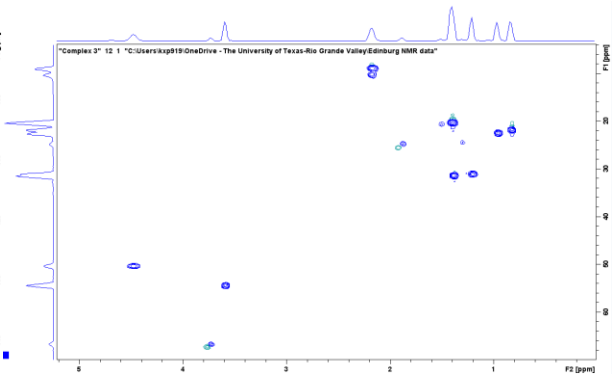

Figure S1-14: ^{1}H NMR spectrum of crude reaction of **2-(PMe$_3$)$_2$** + *i*PrMe in C_6D_6

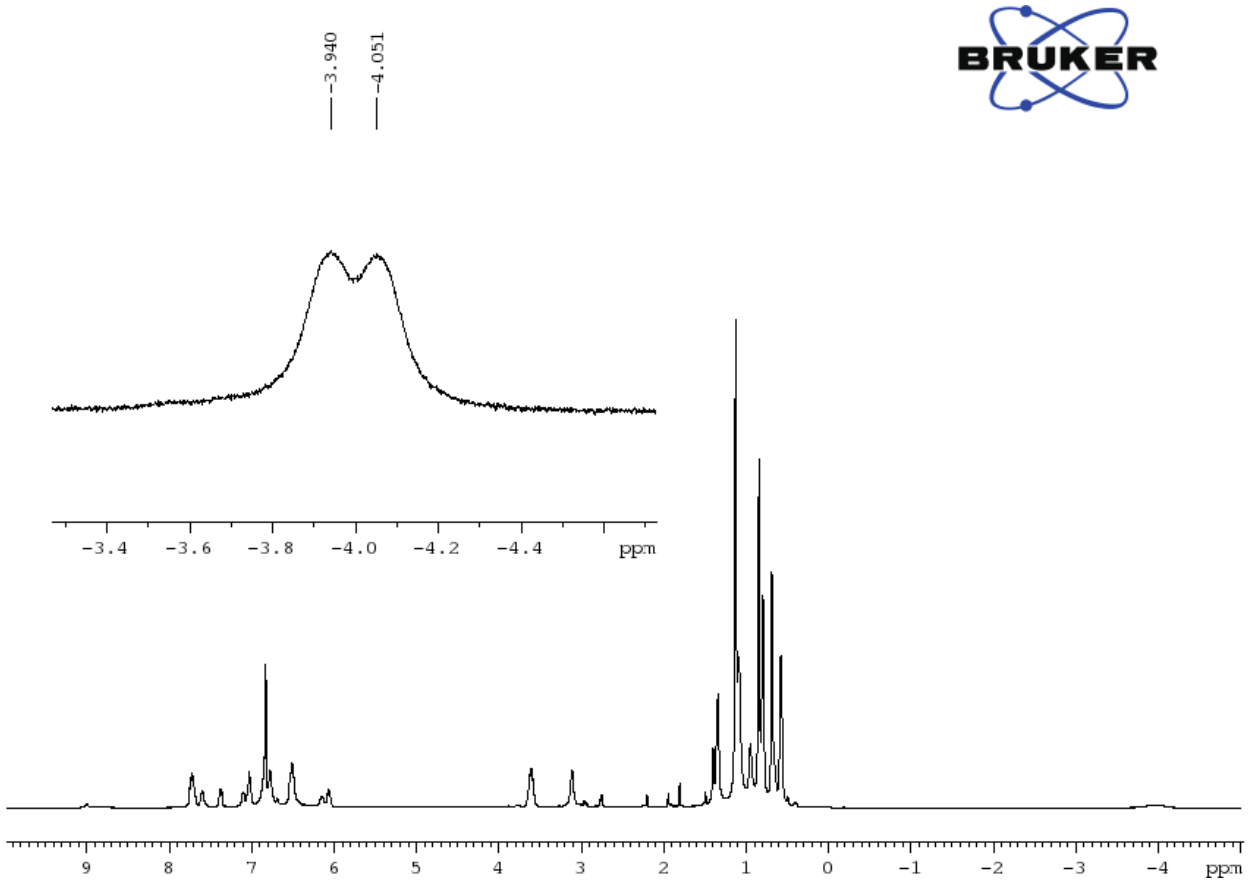

S2: VT NMR spectra

Figure S2-1: Variable Temperature $^{31}P\{^{1}H\}$ NMR spectrum of **Complex 2-(PPh$_3$)$_2$** in C_7D_8

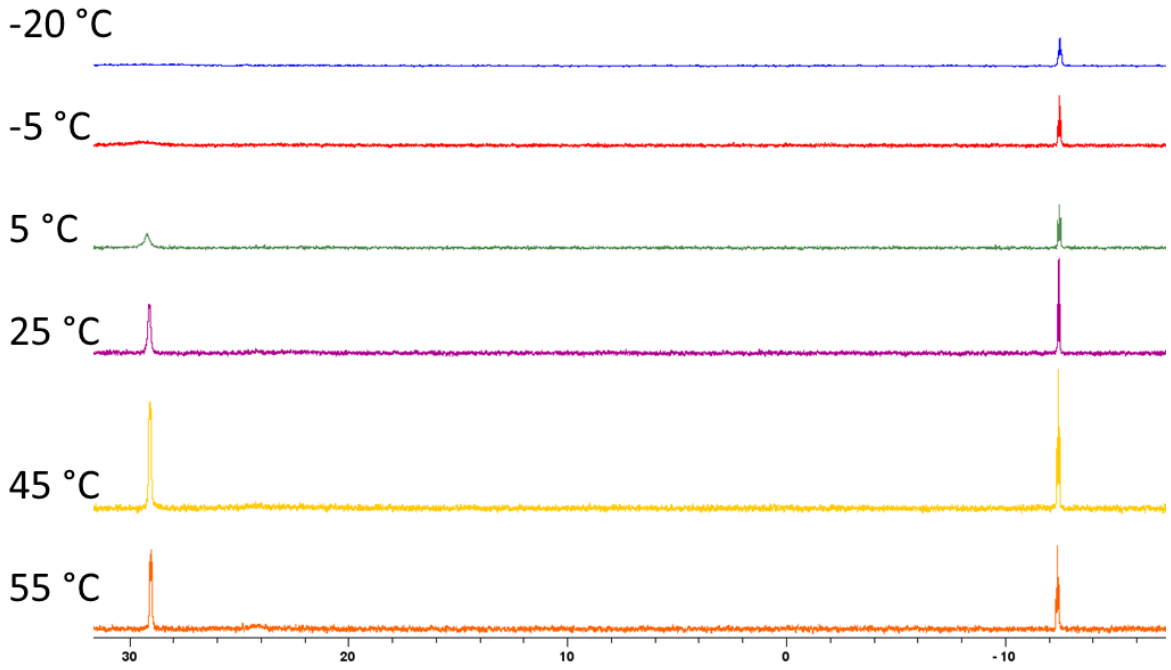

Figure S2-2: Variable Temperature $^{31}P\{^{1}H\}$ NMR spectrum of **Complex 2-(PPh$_3$)$_2$** in C_7D_8

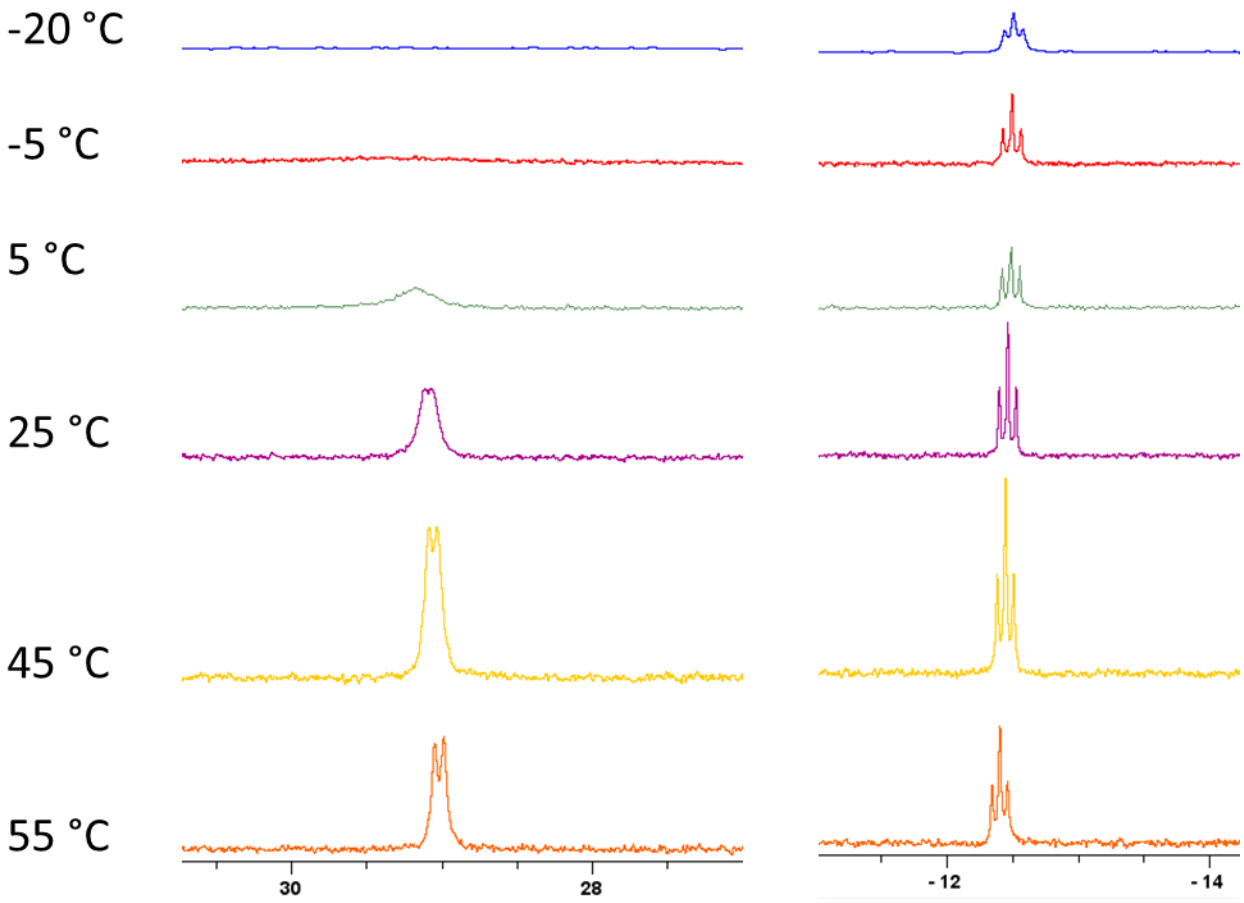

Figure S2-3: Variable Temperature ^{1}H NMR spectrum of **Complex 2-$(PPh_3)_2$** in C_7D_8

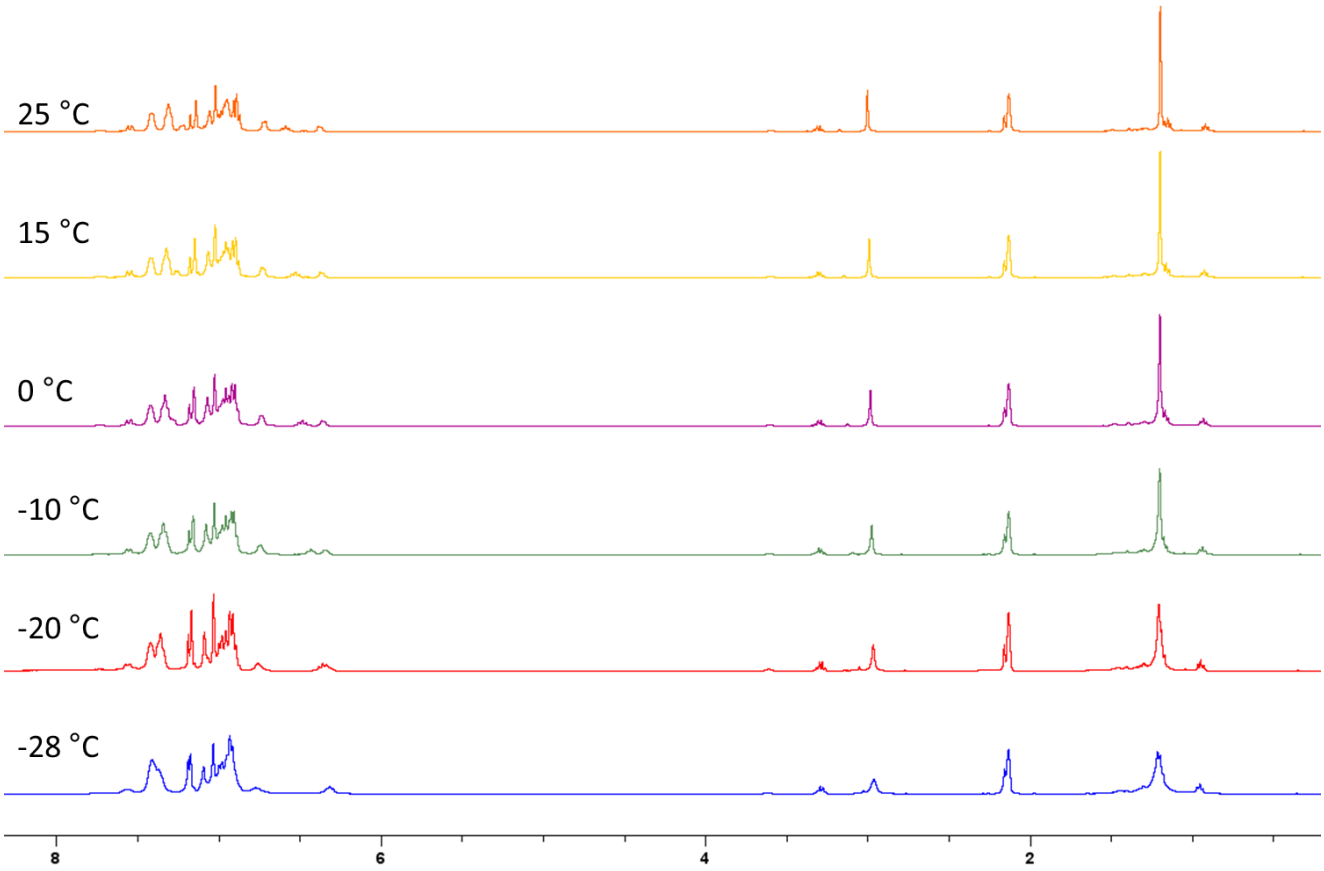

Figure S2-4: Variable Temperature ^{1}H NMR spectrum of **Complex 2-$(PPh_3)_2$** in C_7D_8

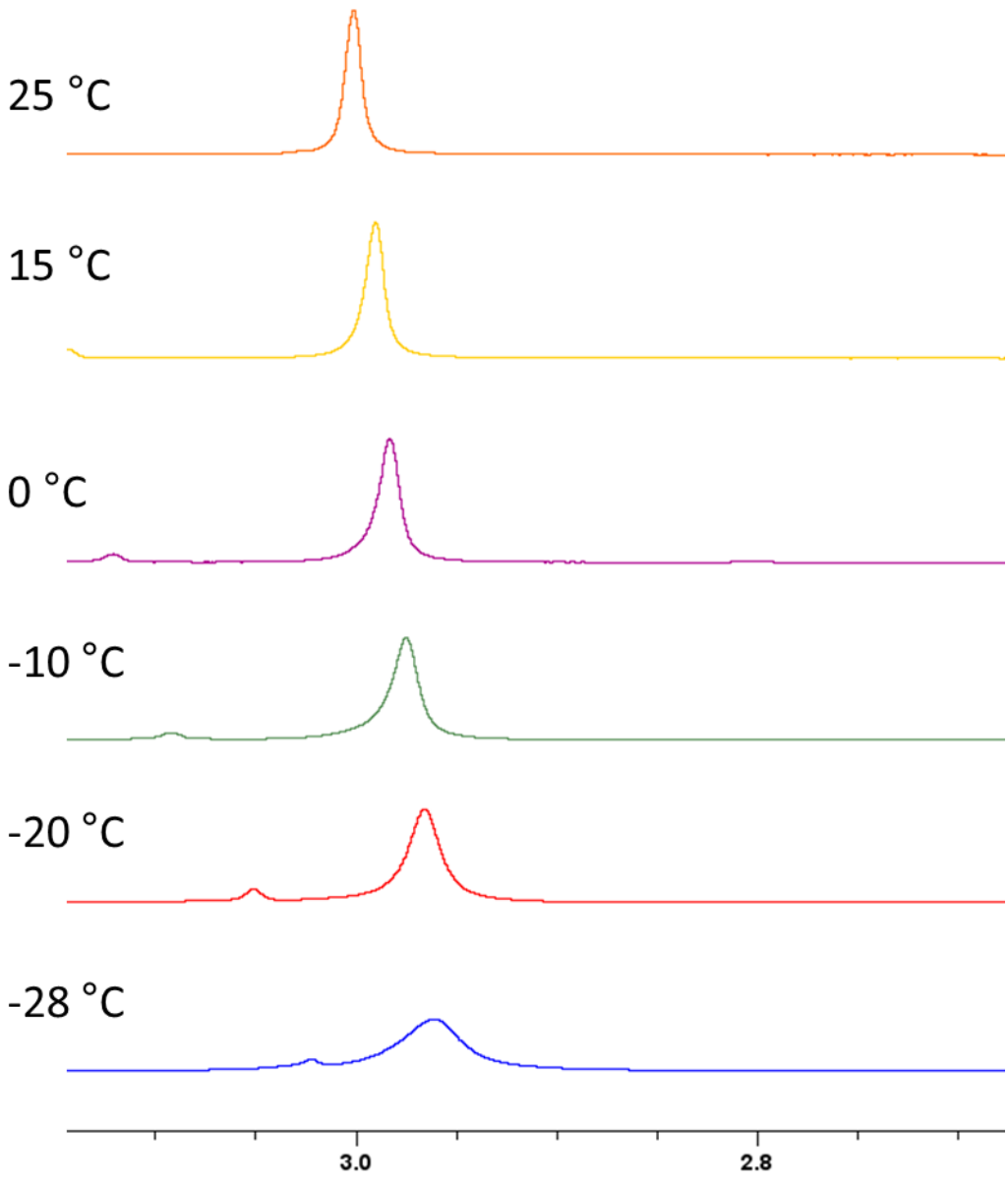

Figure S2-5: Variable Temperature $^{31}P\{^{1}H\}$ NMR spectrum of **Complex 2-(dppm)$_2$** in C_7D_8

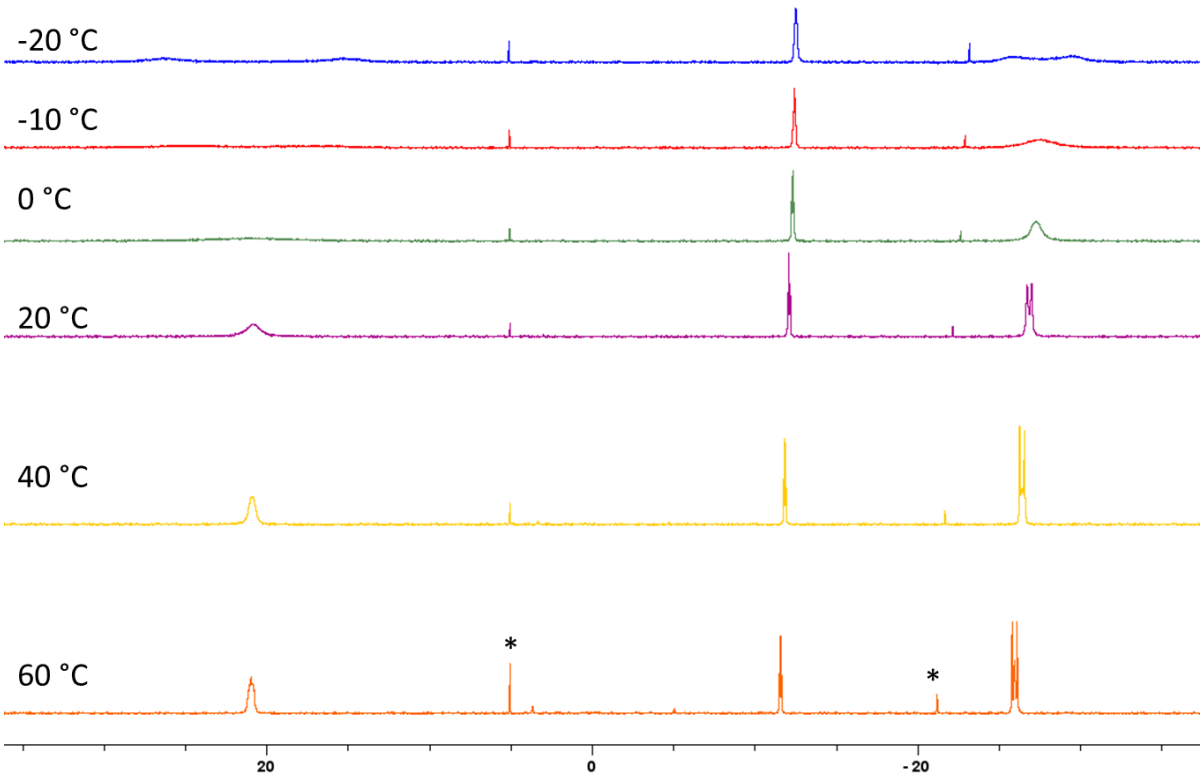

*Impurities that increase in concentration from thermal sensitivity

Figure S2-6: Variable Temperature $^{31}P\{^{1}H\}$ NMR spectrum of **Complex 2-(dppm)$_2$** in C_7D_8

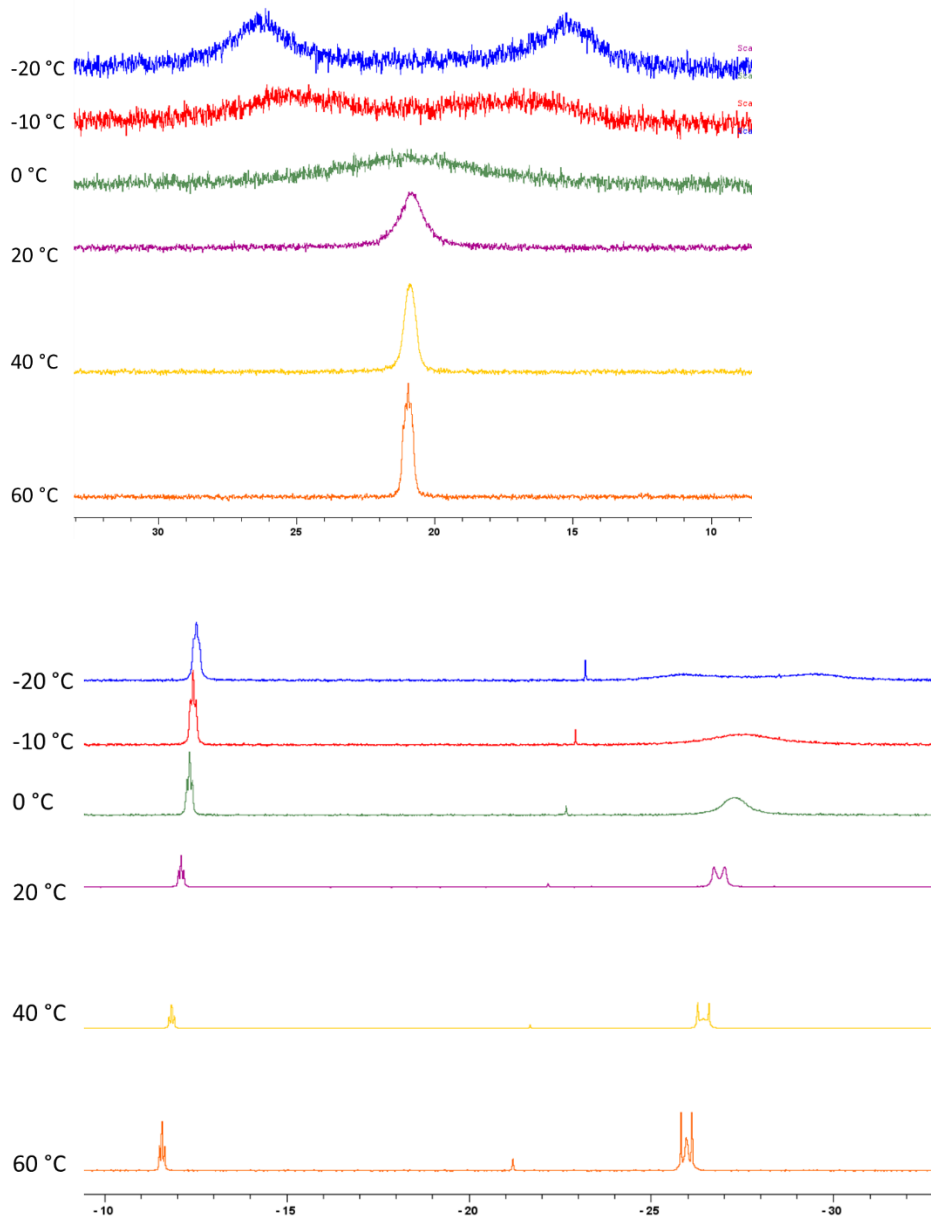

Figure S2-7: $^{31}P\{^{1}H\}$ NMR spectrum of **Complex 2-(dppm)$_2$** in C_7D_8 at 60°C

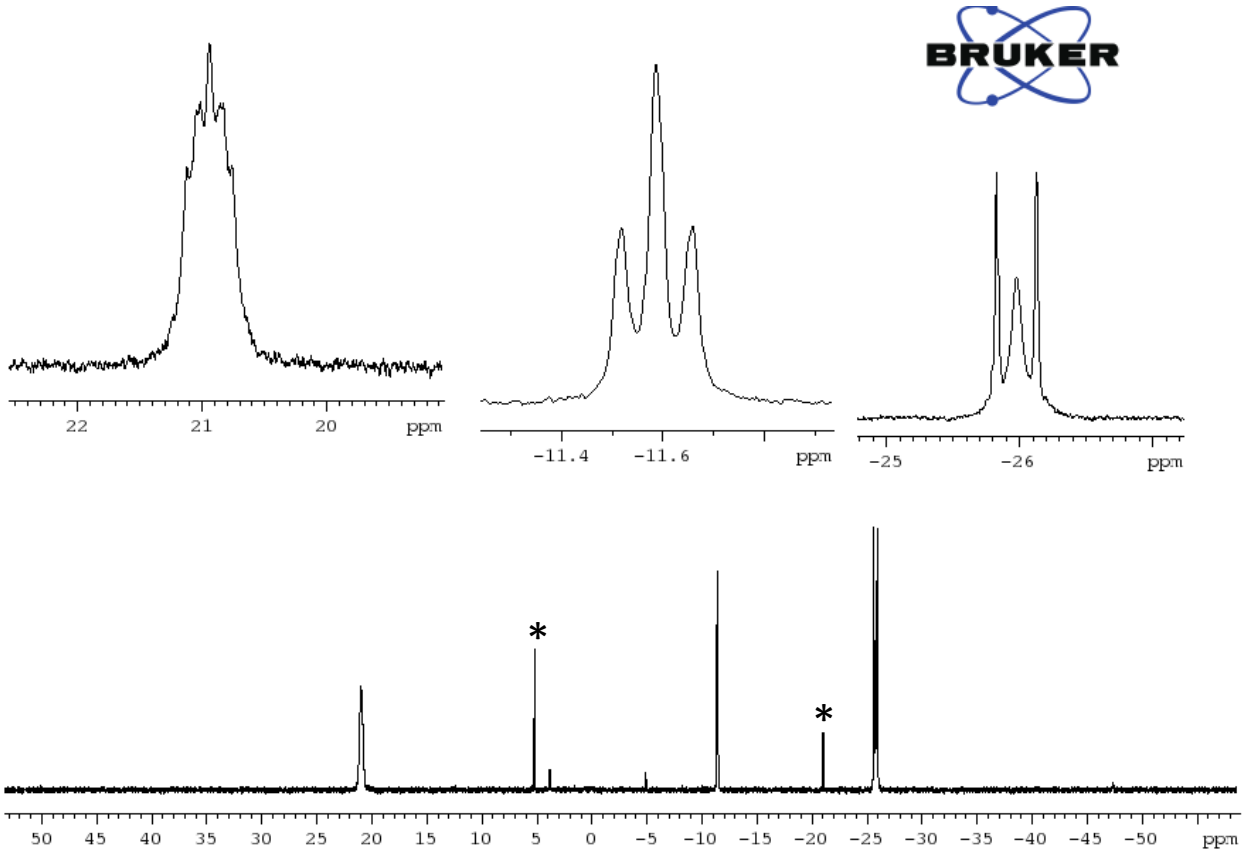

*Impurities generated from thermal sensitivity

S3: Computational Data

Table S3-1: Comparative bond lengths for single-crystal X-ray data and optimized computational data

	1 (Å)		**2-(PPh$_3$)$_2$** (Å)		**2-(dppm)$_2$** (Å)		**2-(PMe$_3$)$_2$** (Å)		**3**(Å)	
	X-ray	Opt.	X-ray	Opt.	X-ray	Opt.	X-ray	Opt.	X-ray	Opt.
Ni-Al	2.3629(7) 2.3683(7)	2.3213 2.3408	2.3222(16)	2.2640	2.269- 2.276(4)	2.2778	2.2503(7) 2.2613(7)	2.2542	2.334(1) 2.336(1)	2.3431
Ni-P1	2.1580(6)	2.1710	2.1832(14)	2.1892	2.169- 2.175(2)	2.2030	2.1410(6) 2.1449(6)	2.1830	2.131(1) 2.133(1)	2.1813
Ni- P2/3	2.1635(6)	2.1677	2.2095(14) 2.1915(16)	2.2168 2.2037	2.171- 2.186(2)	2.1947 2.1774	2.1570(7) 2.1612(7) 2.1674(7) 2.1706(7)	2.1849 2.1794	2.166(1) 2.161(1) 2.156(1) 2.168(1)	2.1700 2.1733
Al-N	1.875(2) 1.879(2) 1.925(3) 1.934(2)	1.8998 1.9649 1.9000 1.9265	1.855(4) 1.866(4)	1.8646 1.8986	1.850- 1.906(6)	1.8722 1.9131	1.854(2) 1.8583(18) 1.8996(17) 1.9041(19)	1.8775 1.9173	1.900(3) 1.901(3) 1.917(3) 1.918(3)	1.9275 1.9515
Al-O	1.997(2) 2.051(2) 2.213(2) 2.226(2)	2.0275 2.0892 2.1483 2.1685	1.937(3)	1.9762	1.916- 1.931(6)	1.9794	1.9302(16) 1.9514(15)	1.9821	1.804(3) 1.806(3)	1.8106
Ni-H	1.57(3) 1.60(3)	1.6266 1.6590	1.54(4)	1.6359	1.43- 1.47(13)	1.6368	1.61(4) 1.67(4)	1.6579	1.19(3) 1.31(3)	1.6205
Al-H	1.59(3) 1.61(3)	1.6999 1.7068	1.74(4)	1.7127	1.55- 1.72(12)	1.7301	1.68(4) 1.71(4)	1.7266	1.88(3) 1.75(3)	1.7341

Table S3-2: Calculated NPA and QTAIM Charges

	Atom/Bond	**1**	**2-(PPh$_3$)$_2$**	**2-(dppm)$_2$**	**2-(PMe$_3$)$_2$**	**3**
QTAIM Charges	Ni	-0.28	-0.16	-0.17	-0.20	-0.16
	Al	+2.36, +2.36	+2.32	+2.31	+2.31	+2.34
	H	-0.58, -0.60	-0.60	-0.59	-0.60	-0.58
NPA Charges	Ni	-1.29	-1.22	-1.27	-1.34	-1.37
	Al	+1.79, +1.77	+1.76	+1.75	+1.72	+1.73
	H	-0.194, -1.99	-0.211	-0.186	-0.175	-0.142

Table S3-3: Molecular Orbitals of **1**

Orbital	Energy Relative to HOMO	
		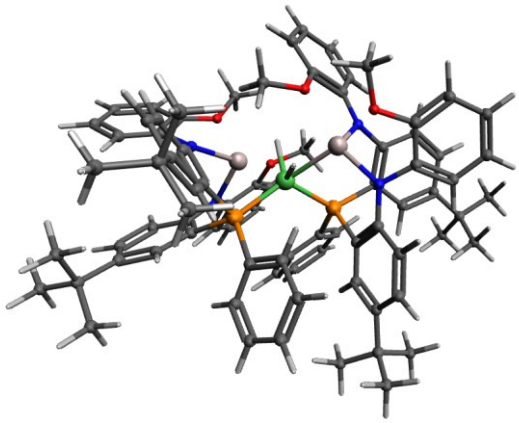

LUMO	+2.195 eV	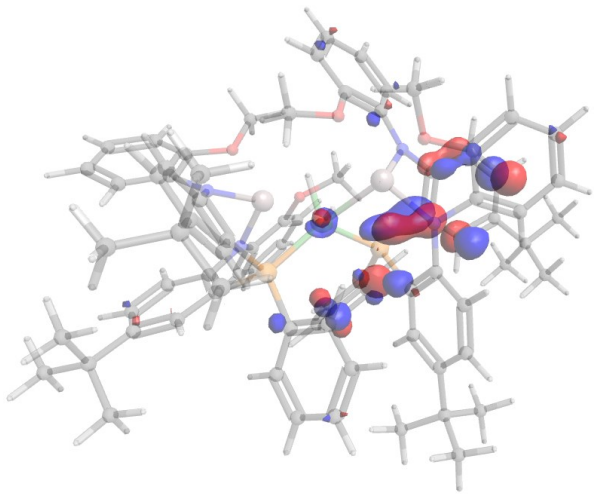
HOMO	0.000 eV	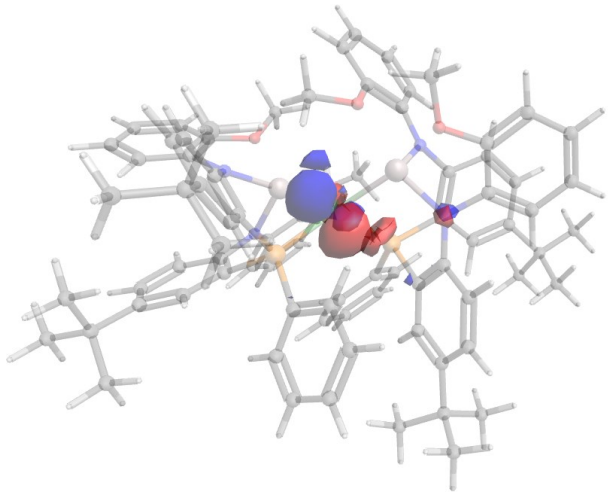
HOMO (-1)	-0.152 eV	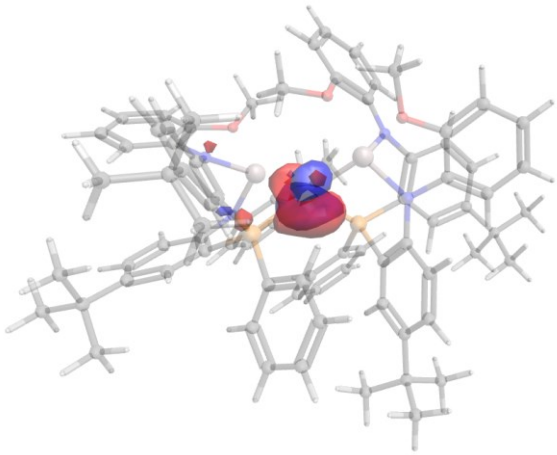

HOMO (-2)	-0.281 eV	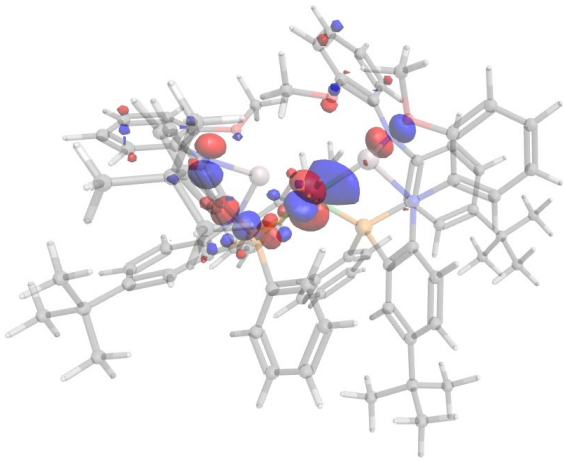
HOMO (-3)	-0.606 eV	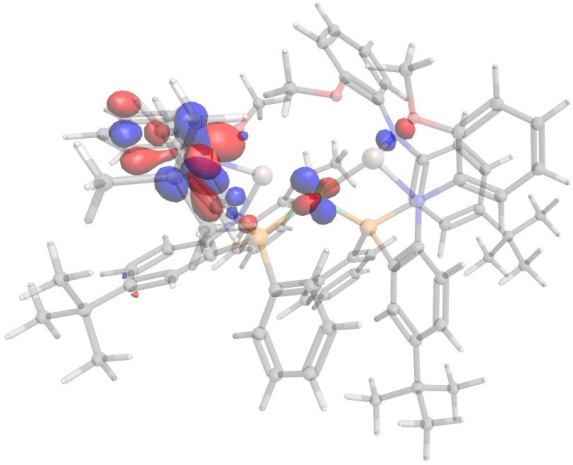
HOMO (-4)	-0.633 eV	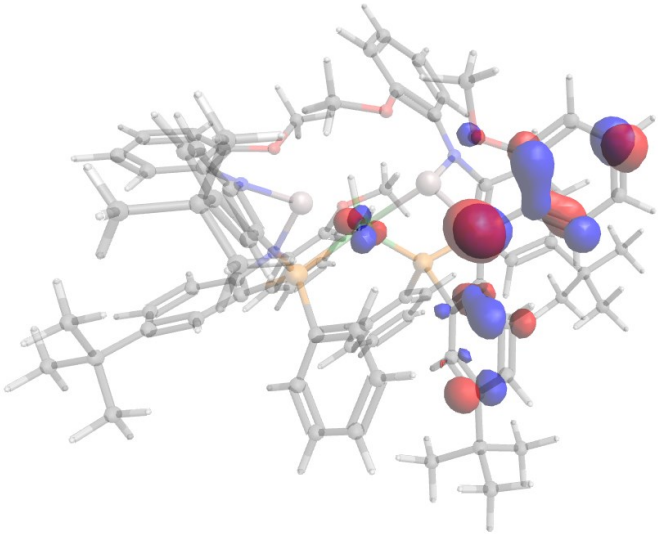

HOMO (-5)	-0.684 eV	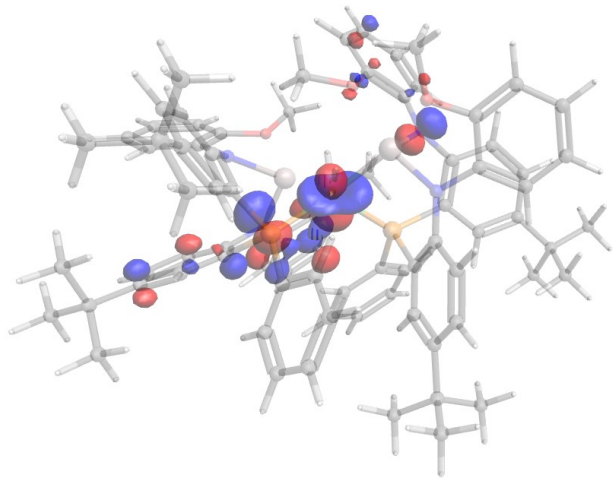
HOMO (-6)	-0.919 eV	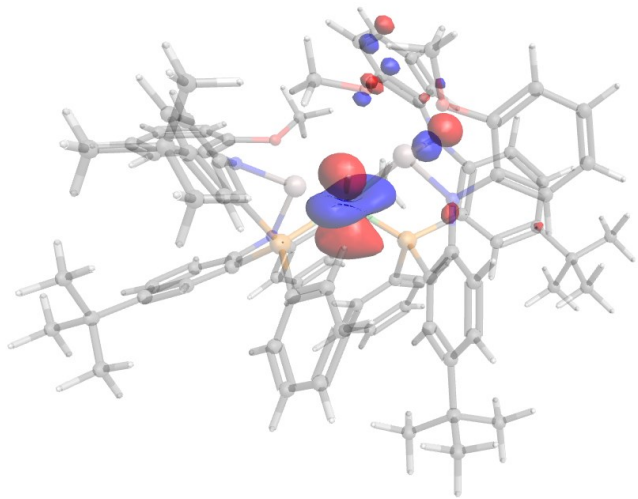
HOMO (-7)	-1.128 eV	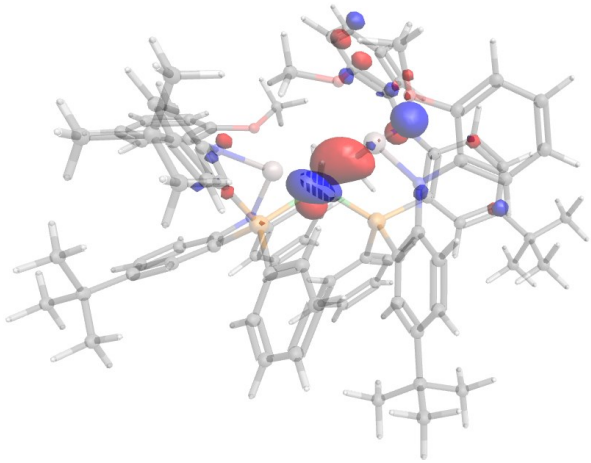

HOMO (-8)	-1.423 eV	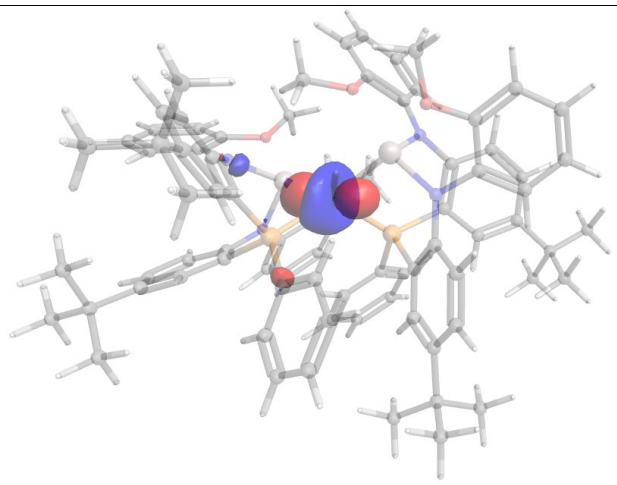
HOMO (-9)	-1.777 eV	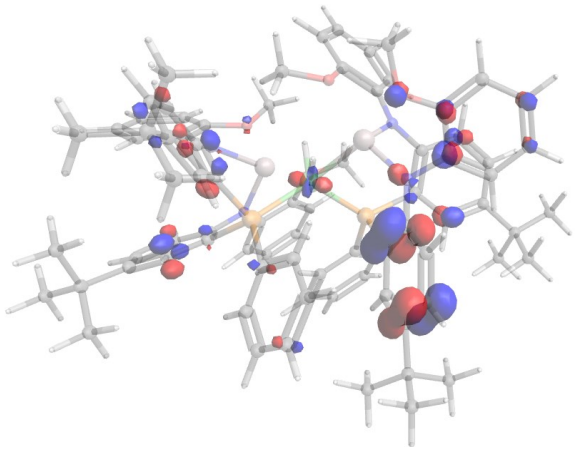
HOMO (-10)	-1.790 eV	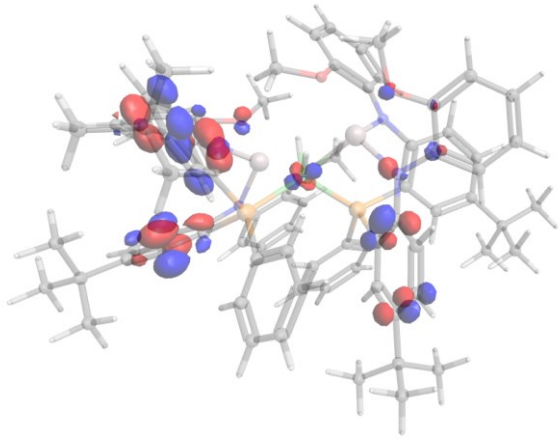

Table S3-4: Molecular Orbitals of **2-(PPh$_3$)$_2$**

Orbital	Energy Relative to HOMO	Molecular Orbital Images
		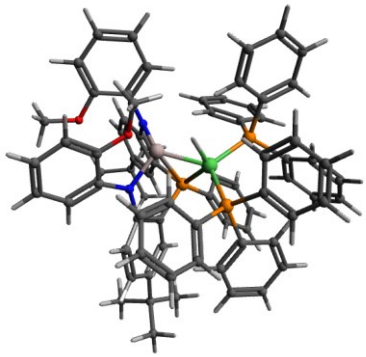
LUMO	+2.157 eV	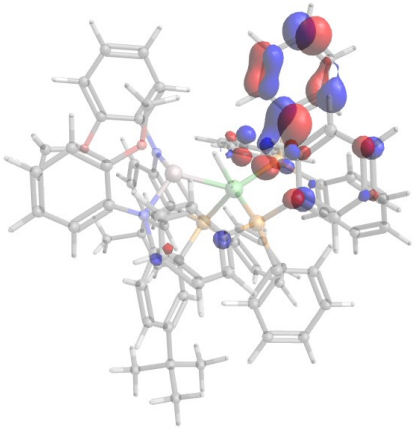
HOMO	0.000 eV	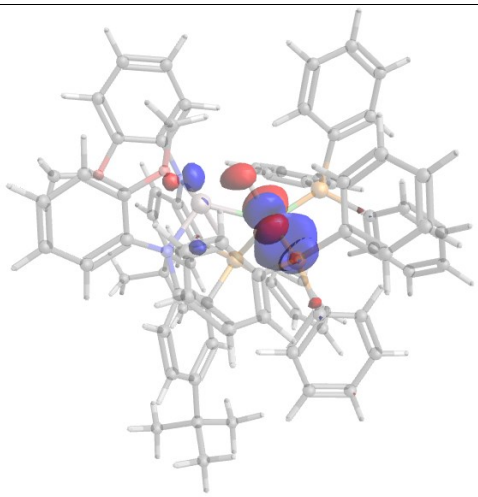

HOMO (-1)	-0.166 eV	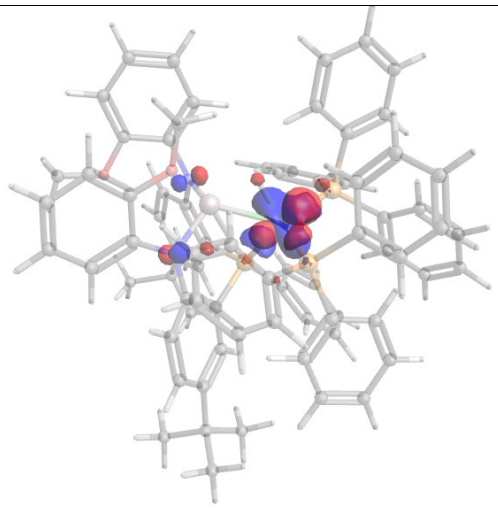
HOMO (-2)	-0.315 eV	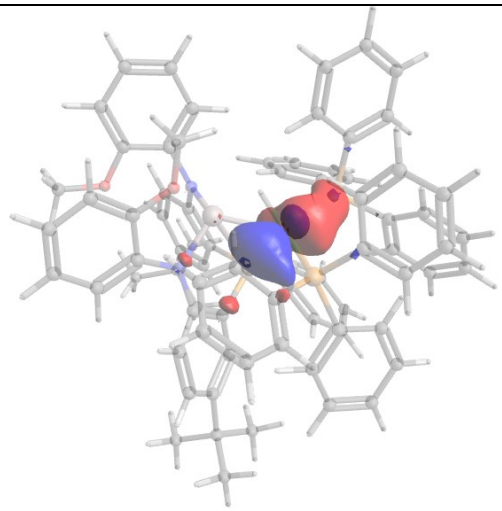
HOMO (-3)	-0.484 eV	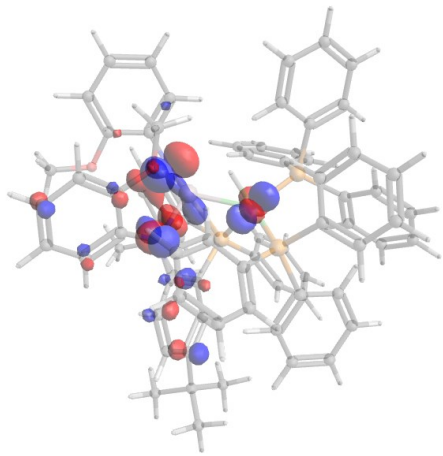

HOMO (-4)	-0.672 eV	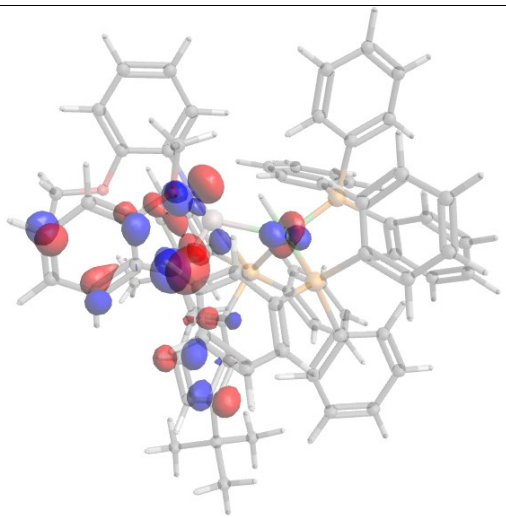
HOMO (-5)	-0.927 eV	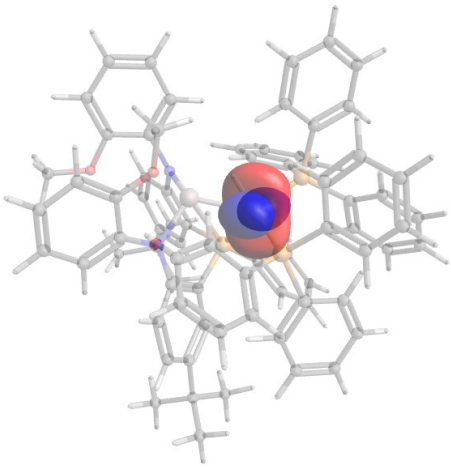
HOMO (-6)	-1.287 eV	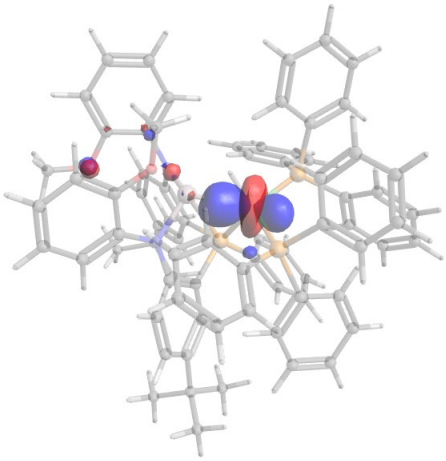

HOMO (-7)	-1.551 eV	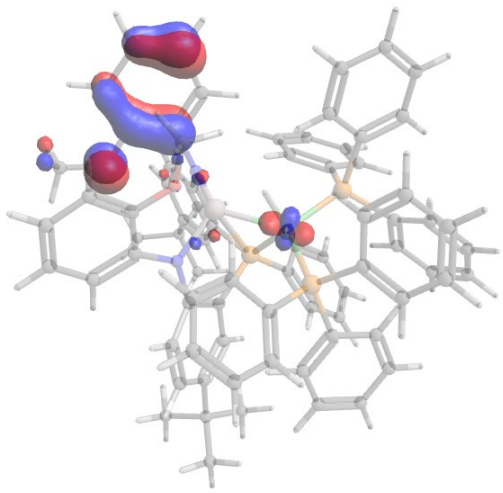
HOMO (-8)	-1.698 eV	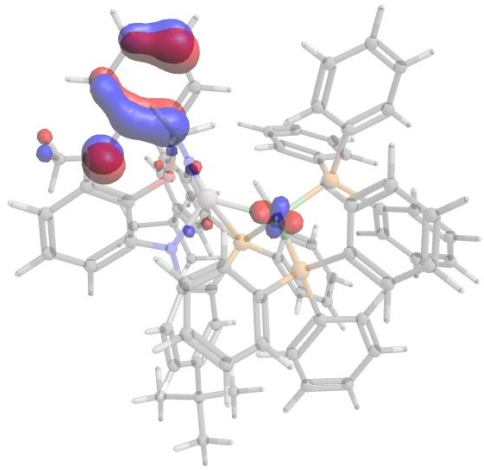
HOMO (-9)	-1.939 eV	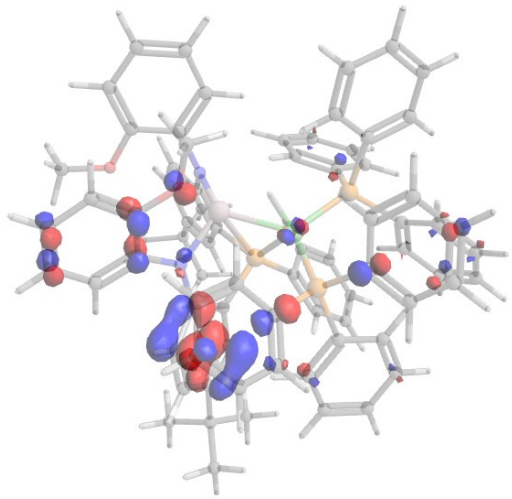

HOMO (-10)	-1.946 eV	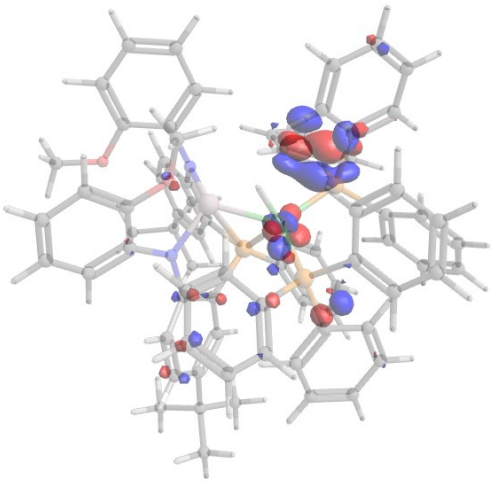

Table S3-5: Molecular Orbitals of **2-(dppm)$_2$**

Orbital	Energy Relative to HOMO	
		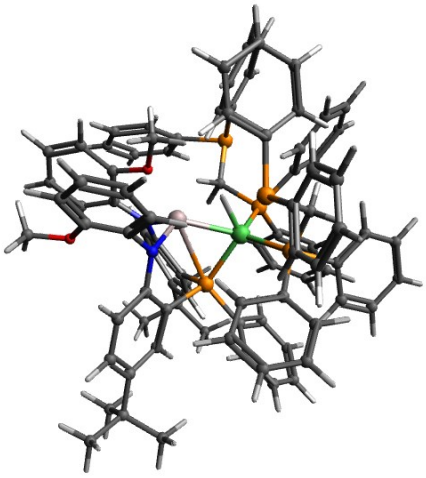

LUMO	+2.006 eV	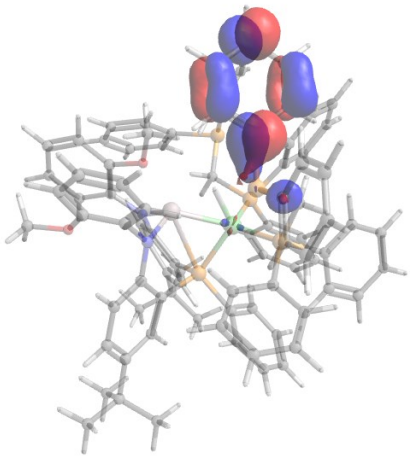
HOMO	0.000 eV	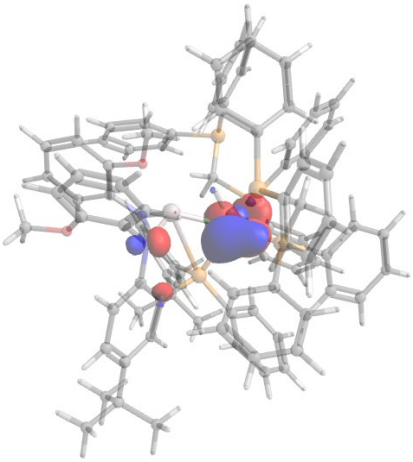
HOMO (-1)	-0.080 eV	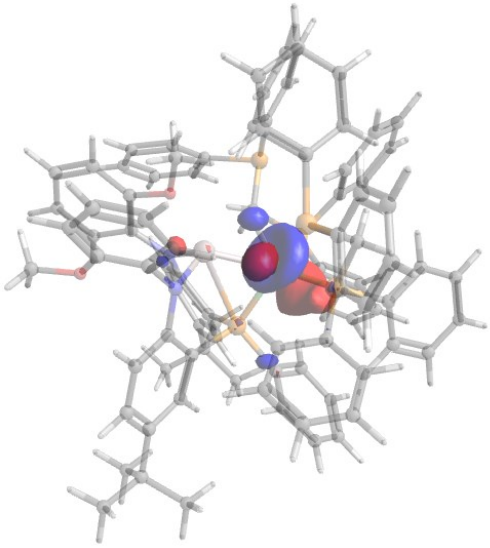

HOMO (-2)	-0.257 eV	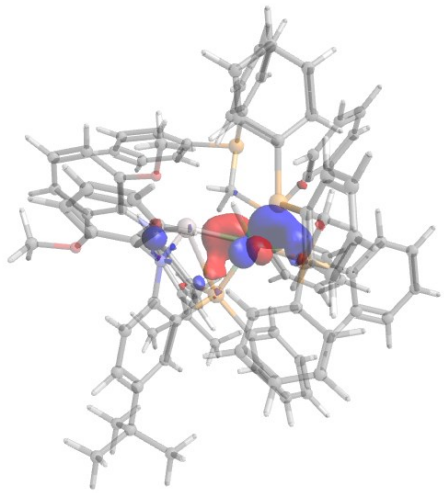
HOMO (-3)	-0.406 eV	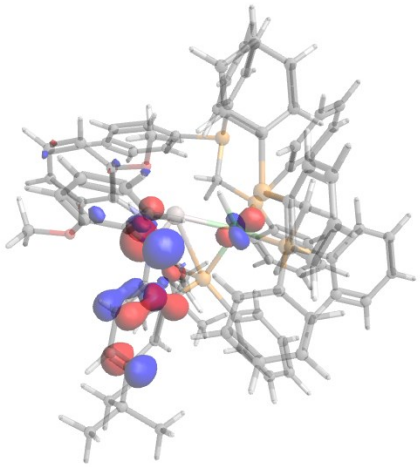
HOMO (-4)	-0.613 eV	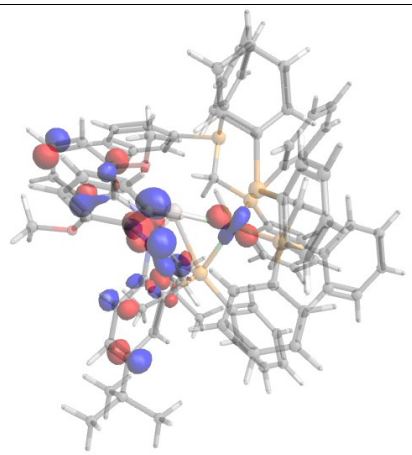

HOMO (-5)	-0.905 eV	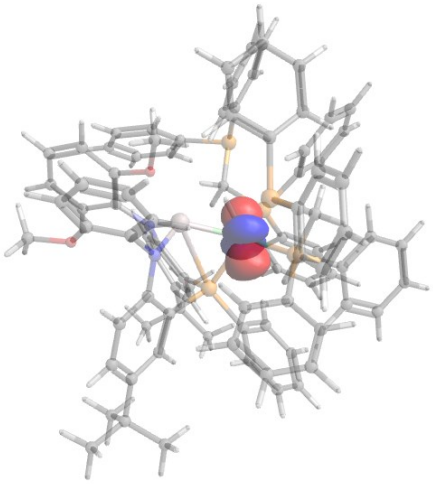
HOMO (-6)	-1.237 eV	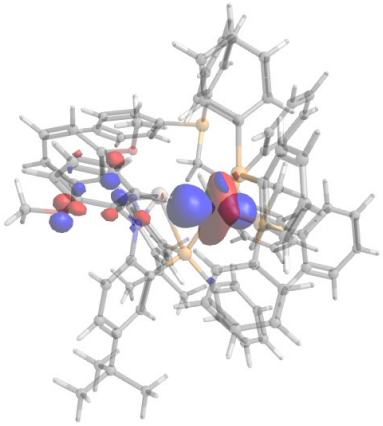
HOMO (-7)	-1.398 eV	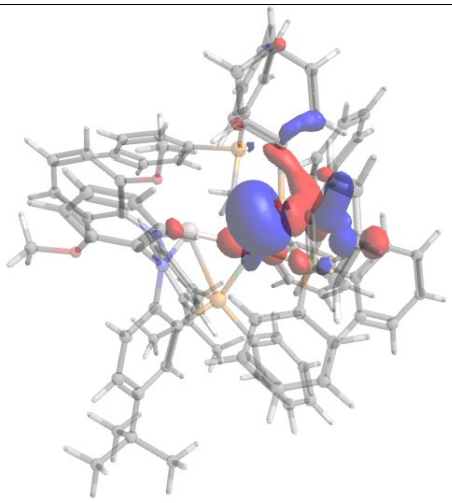

HOMO (-8)	-1.443 eV	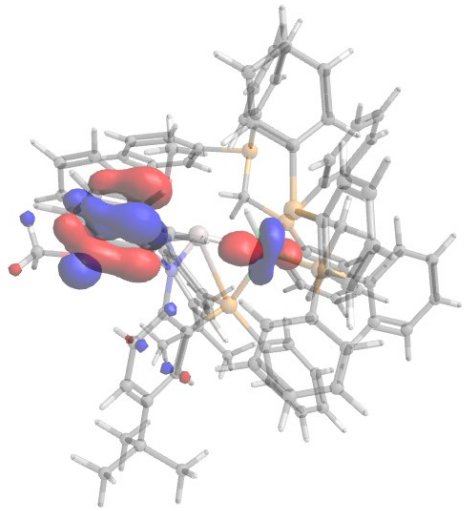
HOMO (-9)	-1.478 eV	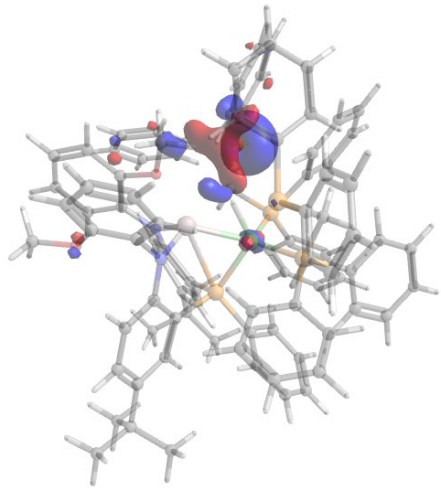
HOMO (-10)	-1.647 eV	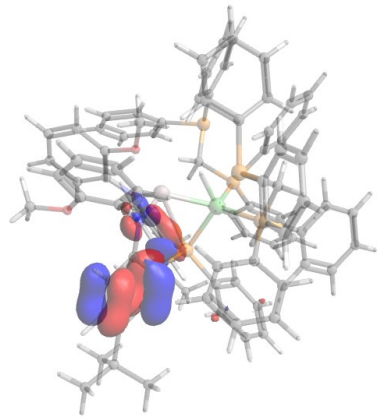

Table S3-6: Molecular Orbitals of **2-(PMe$_3$)$_2$**

Orbital	Energy Relative to HOMO	Molecular Orbital Images
		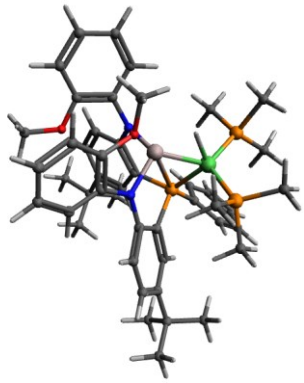
LUMO	+2.130 eV	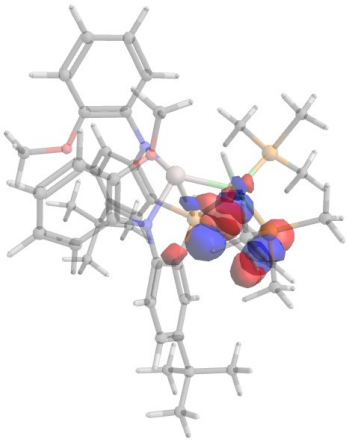
HOMO	0.000 eV	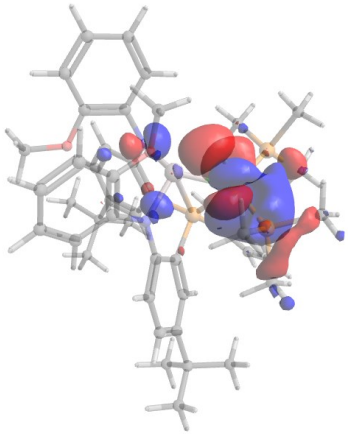

HOMO (-1)	-0.142 eV	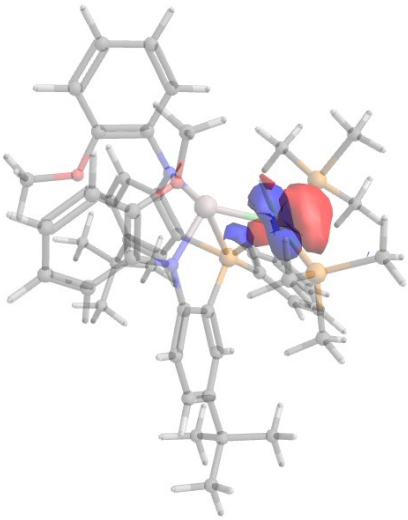
HOMO (-2)	-0.311 eV	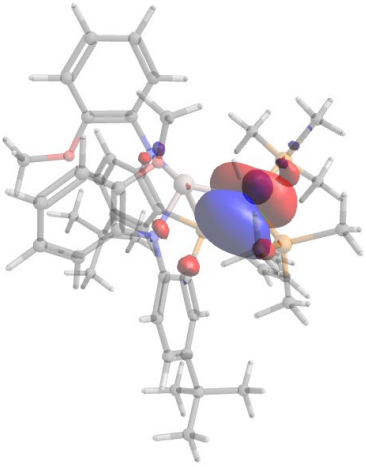
HOMO (-3)	-0.574 eV	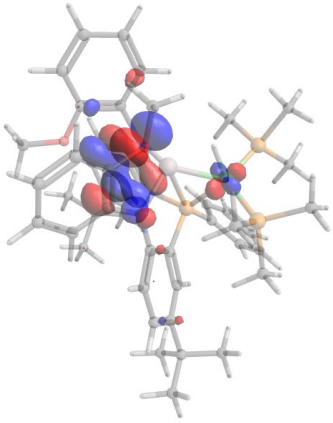

HOMO (-4)	-0.769 eV	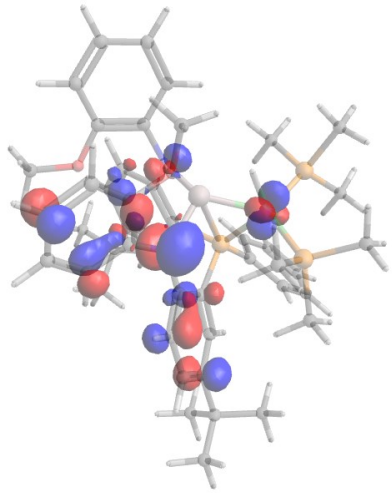
HOMO (-5)	-0.963 eV	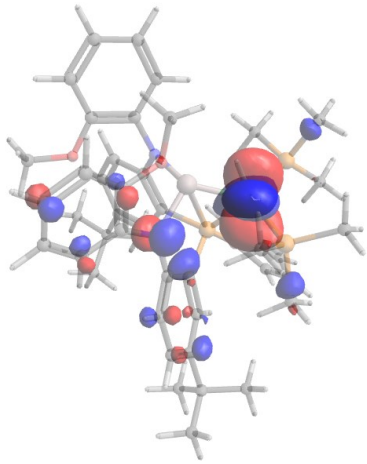
HOMO (-6)	-1.300 eV	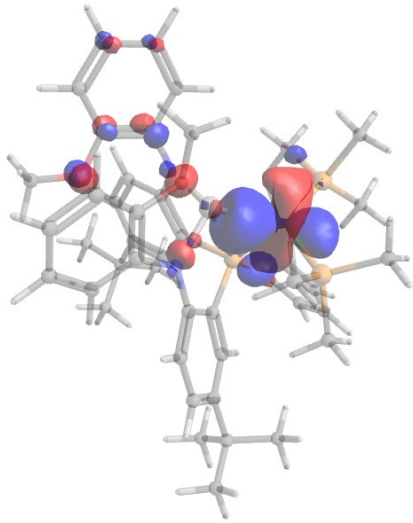

HOMO (-7)	-1.650 eV	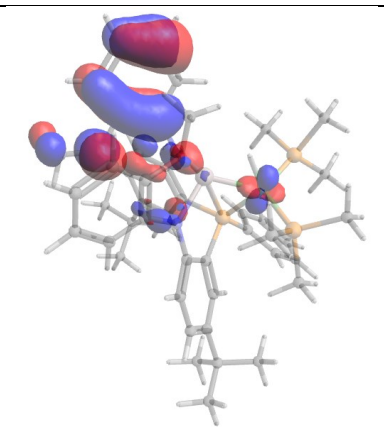
HOMO (-8)	-1.876 eV	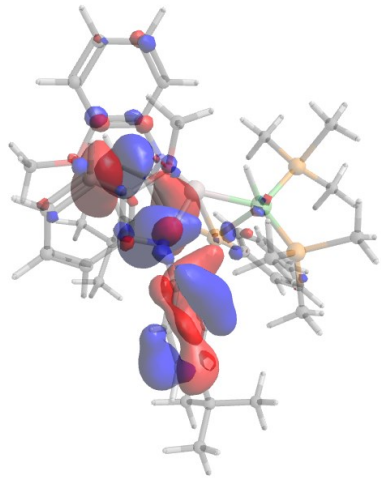
HOMO (-9)	-2.167 eV	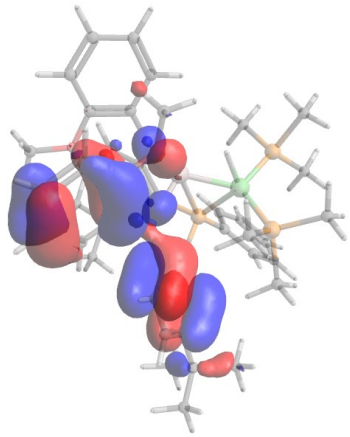

HOMO (-10)	-2.313 eV	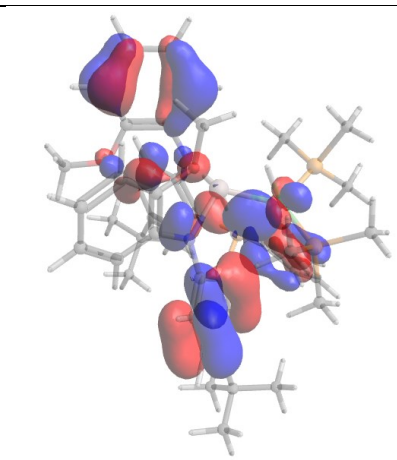

Table S3-7: Molecular Orbitals of **3**

Orbital	Energy Relative to HOMO	Molecular Orbital Images
		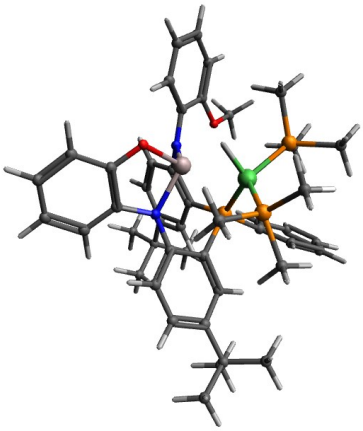

LUMO	+1.684 eV	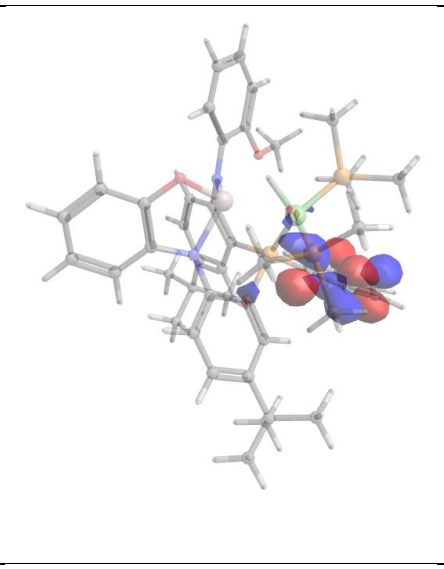
HOMO	0.000 eV	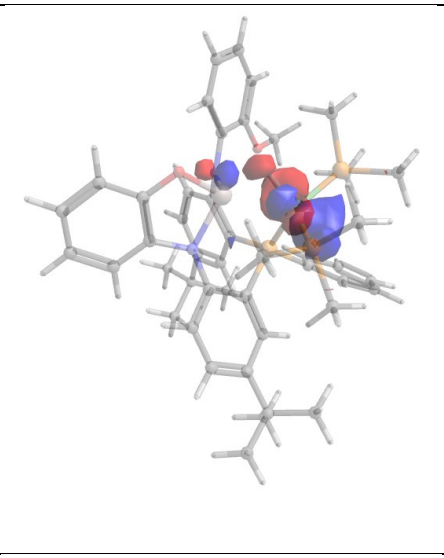
HOMO (-1)	-0.146 eV	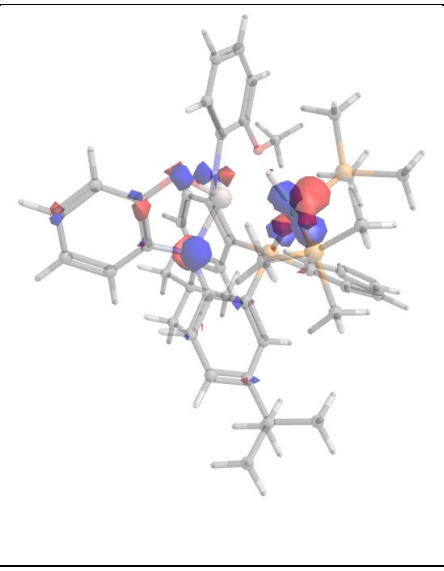

HOMO (-2)	-0.328 eV	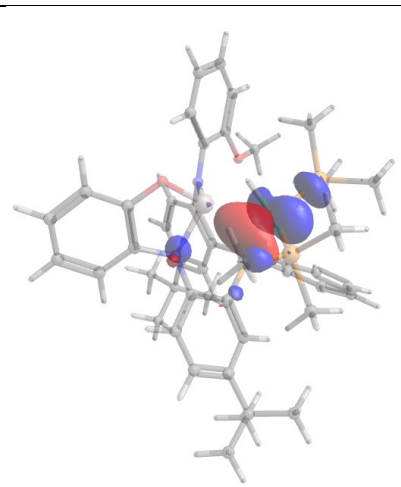
HOMO (-3)	-0.407 eV	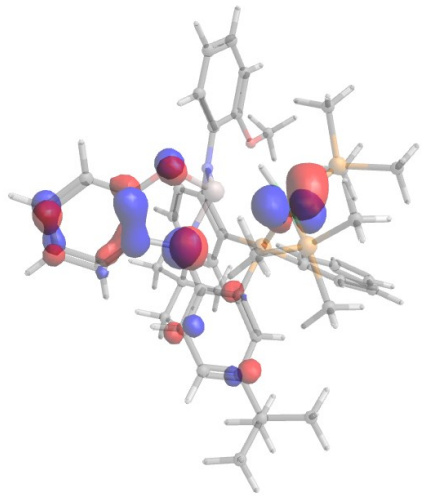
HOMO (-4)	-0.717 eV	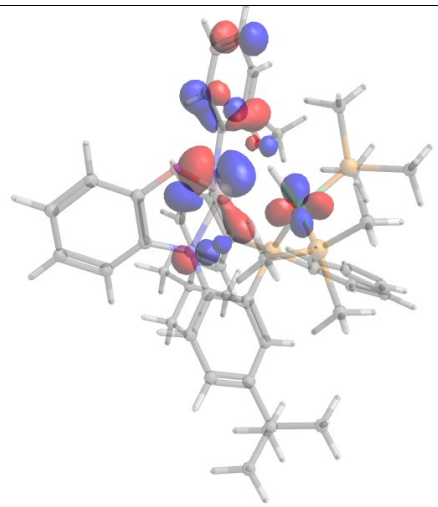

HOMO (-5)	-0.985 eV	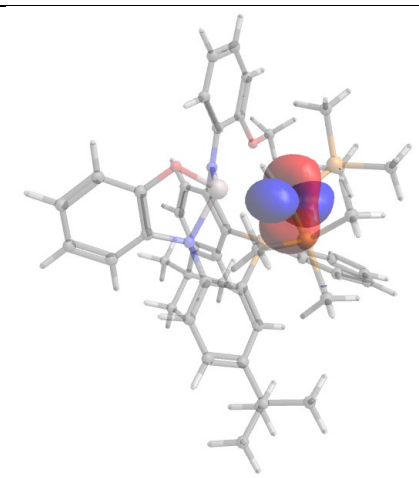
HOMO (-6)	-1.241 eV	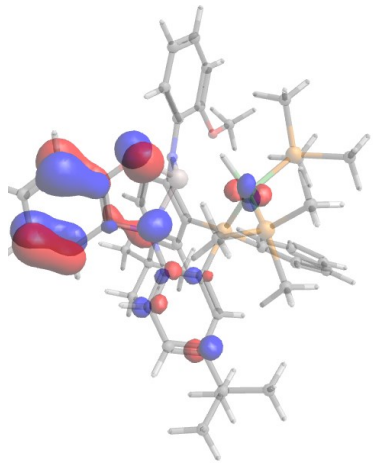
HOMO (-7)	-1.298 eV	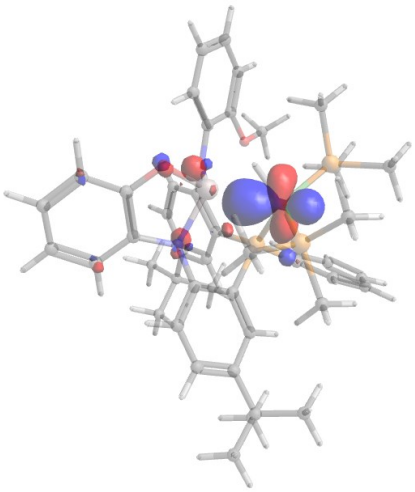

HOMO (-8)	-1.820 eV	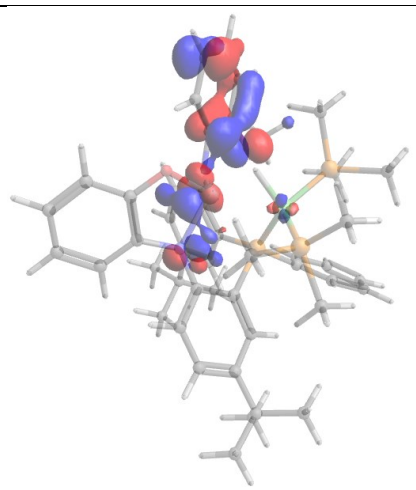
HOMO (-9)	-2.035 eV	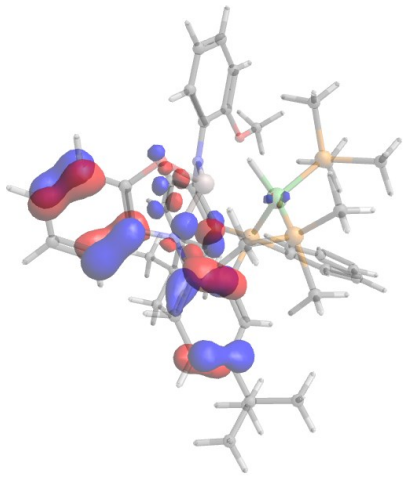
HOMO (-10)	-2.285 eV	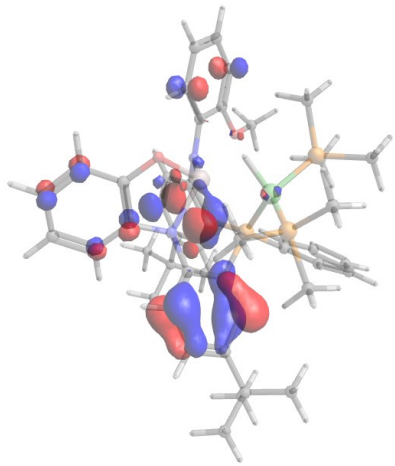

Table S3-8: DFT Calculated Hydricity in Acetonitrile

Complex	**Hydricity (kcal/mol)**
1	57.9, 61.9
2-$(PPh_3)_2$	59.3
2-$(dppm)_2$	59.8
2-$(PMe_3)_2$	54.1
3	40.1

S4: Crystallography

Crystallography. Complete details of the structures can be obtained from the Cambridge Crystallographic Data Centre at www.ccdc.cam.ac.uk. The CCDC accession numbers for the reported complexes are 2362005, 2362006, 2362008, and 2362009.

X-ray images from Mercury for heterobimetallic complex 2-$(PPh_3)_2$

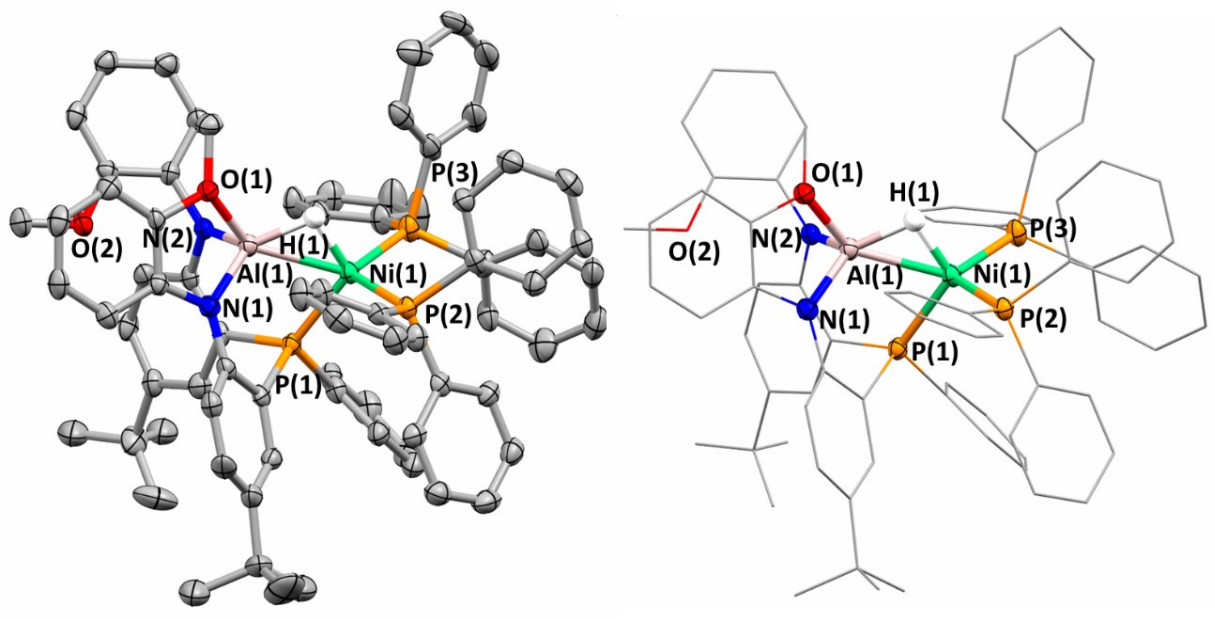

Special Refinement Details of heterobimetallic complex 2-$(PPh_3)_2$:

Single crystals of $C_{76}H_{65}AlN_2NiO_2P_3$ (**2-$(PPh_3)_2$**) were prepared by vapor diffusion benzene/pentane. Suitable crystals of each sample were mounted in polybutene oil in a nitrogen glovebox, transferred to a nylon loop, and then quickly placed to the goniometer head of a Rigaku XtaLAB Synergy-S Dualflex, HyPix Arc-150 diffractometer with CuKα radiation (λ = 1.54184 Å). All data was collected at 100.15 K. Data collection and unit cell refinement were performed using *CrysAlisPro*[1] software. Data processing and absorption correction were accomplished with *CrysAlisPro* and *SCALE3 ABSPACK*,[2] respectively. The structure was solved with the ShelXT[3] structure solution program using direct methods and Olex2[4] as the graphical interface. The model was refined with ShelXL[5] using full-matrix, least squares minimization. SQUEEZE was used to supress two sections of electron density likely corresponding to two highly disordered molecules of benzene. All non-hydrogen atoms were refined with anisotropic displacement parameters. The

hydrogen atom attached to the aluminum and nickel ion, was determined by electron density plot. All other hydrogen atom positions were determined by geometry and refined by a riding model.

X-ray images from Mercury for heterobimetallic complex 2-(dppm)$_2$

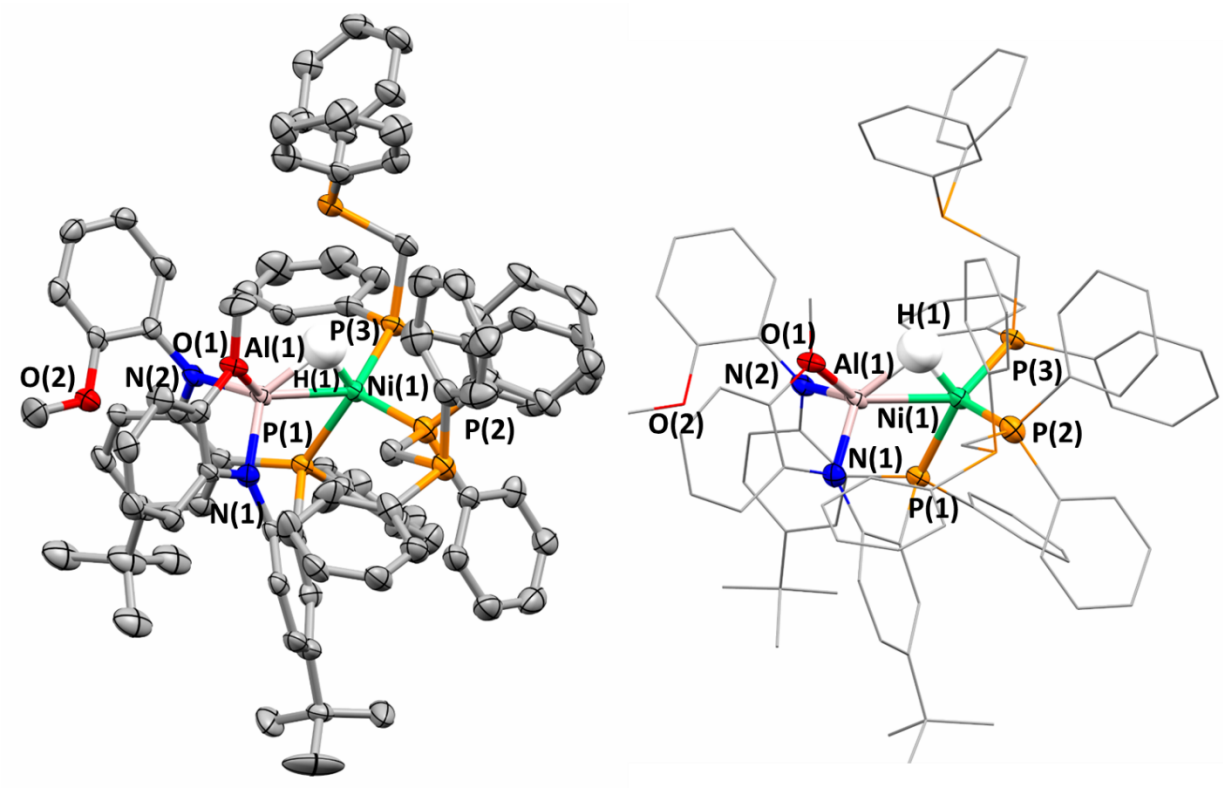

Special Refinement Details of heterobimetallic complex2-(dppm)$_2$:

Single crystals of $C_{102}H_{99}AlN_2NiO_2P_5$(**2-(dppm)$_2$**) were prepared by slow evaporation of a benzene solution. A suitable dark yellow plate-like crystal, with dimensions of 0.310 mm × 0.110 mm × 0.060 mm, was mounted in paratone oil onto a nylon loop. All data were collected at 100.0(1) K, using a XtaLAB Synergy/ Dualflex, HyPix fitted with CuKα radiation (λ = 1.54184 Å). Data collection and unit cell refinement were performed using *CrysAlisPro* software.[1] The total number of data were measured in the 5.6° < 2θ < 153.8° using ω scans. Data processing and absorption correction, giving minimum and maximum transmission factors (0.559, 1.000) were accomplished with *CrysAlisPro*[1] and *SCALE3 ABSPACK*,[2] respectively. The structure, using *Olex2*[4], was solved with the ShelXT[3] structure solution program using direct methods and refined (on F2) with the ShelXL[5] refinement package using full-matrix, least-squares techniques. All non-

hydrogen atoms were refined with anisotropic displacement parameters The hydrogen atom attached to the aluminum and nickel ion, was determined by electron density plot. All other hydrogen atom positions were determined by geometry and refined by a riding model. A solvent mask was performed to remove disordered solvent molecules (4 benzene molecules) from the crystal lattice. PLATON was used to search for a higher symmetry space group, but no obvious space group was found.

X-ray images from Mercury for heterobimetallic complex 2-$(PMe_3)_2$

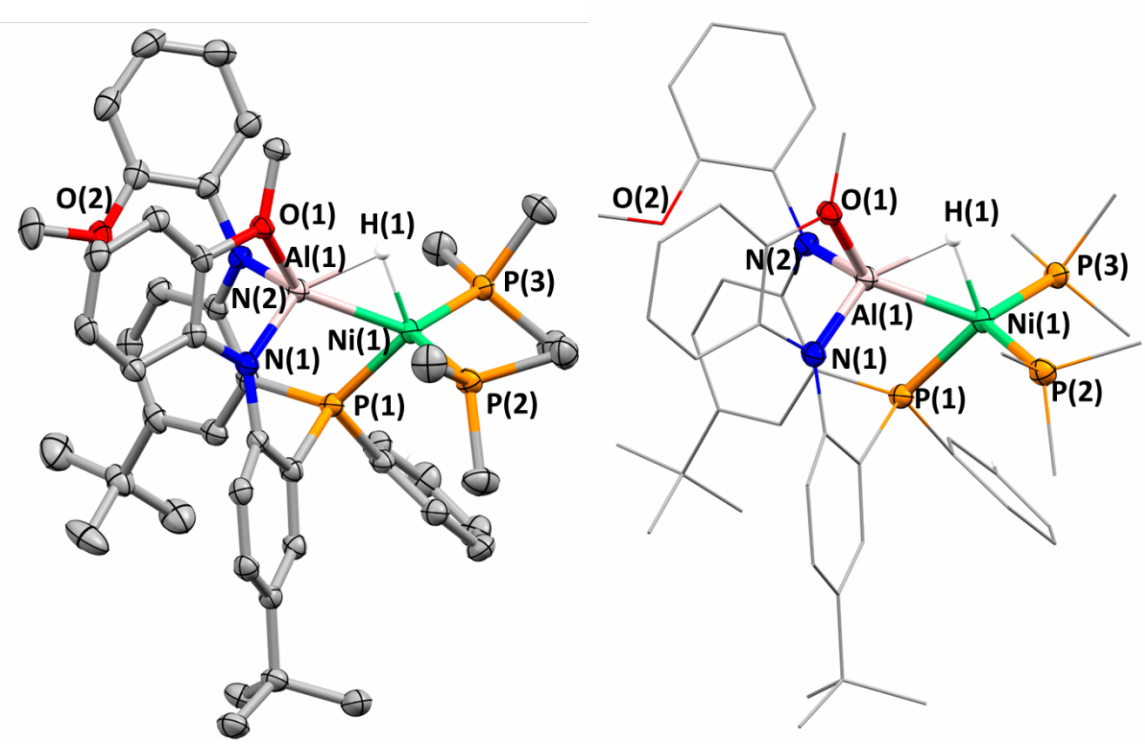

Special Refinement Details of heterobimetallic complex 2-$(PMe_3)_2$:

Single crystals of $C_{46}H_{58}AlN_2NiO_2P_3$ (**2-$(PMe_3)_2$**) were prepared by slow evaporation of diethyl ether. Suitable crystals of each sample were mounted in polybutene oil in a nitrogen glovebox, transferred to a nylon loop, and then quickly placed to the goniometer head of a Rigaku XtaLAB Synergy-S Dualflex, HyPix Arc-150 diffractometer with CuKα radiation (λ = 1.54184 Å). All data was collected at 100.15 K. Data collection and unit cell refinement were performed using *CrysAlisPro*[1] software. Data processing and absorption correction were accomplished with *CrysAlisPro* and *SCALE3 ABSPACK*[2], respectively. The structure was solved with the ShelXT[4] structure solution program using direct methods and Olex2[3] as the graphical interface. The model was refined with ShelXL[5] using full-matrix, least squares minimization. The hydrogen atom

attached to the aluminum and nickel ion, was determined by electron density plot. All other hydrogen atom positions were determined by geometry and refined by a riding model.

X-ray images from Mercury for heterobimetallic complex 3

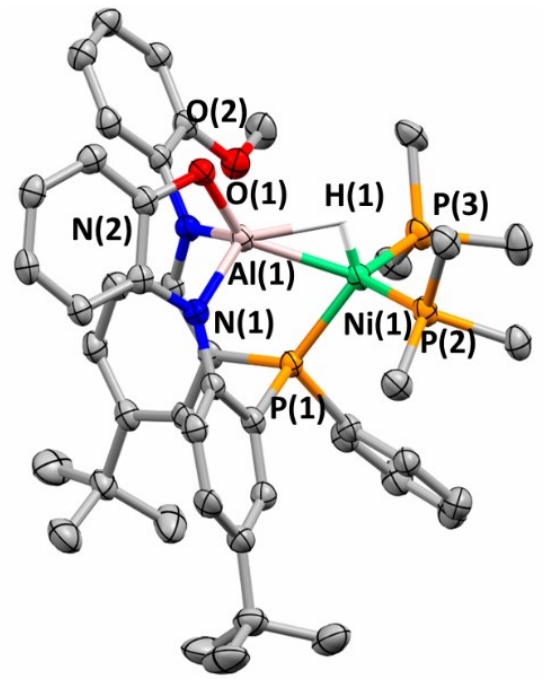

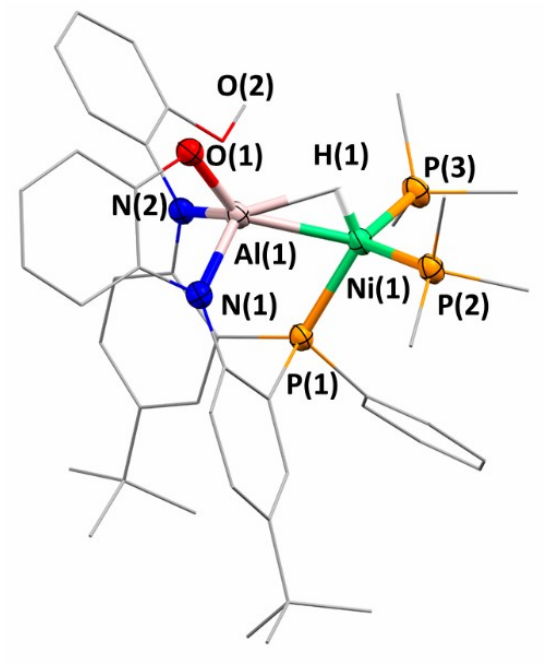

Special Refinement Details of Complex 3:

Single crystals of $C_{65}H_{97}AlN_4NiO_4P_3$(**3**) were prepared by slow evaporation of hexamethyldisiloxane into a THF solution. A suitable dark yellow block-like crystal, with dimensions of 0.273 mm × 0.128 mm × 0.102 mm, was mounted in paratone oil onto a nylon loop. All data were collected at 100.0(1) K and 298(1) K, using a XtaLAB Synergy/ Dualflex, HyPix fitted with CuKα radiation (λ = 1.54184 Å). Data collection and unit cell refinement were performed using *CrysAlisPro* software.[1] The total number of data were measured in the 5.4° < 2θ < 153.0° for compound (**3**) using ω scans. Data processing and absorption correction, giving minimum and maximum transmission factors (0.177, 1.000 for compound (3)) were accomplished

with *CrysAlisPro*[1] and *SCALE3 ABSPACK*[2], respectively. The structure, using *Olex2*[4], was solved with the ShelXT[3] structure solution program using direct methods and refined (on F2) with the ShelXL[5] refinement package using full-matrix, least-squares techniques. All non-hydrogen atoms were refined with anisotropic displacement parameters. The hydrogen atom attached to the aluminum and nickel ion, was determined by electron density plot. All other hydrogen atom positions were determined by geometry and refined by a riding model.

Table S4-1: Crystallographic Information of Heterobimetallic Complexes

Compound	**2-(PPh$_3$)$_2$**	**2-(dppm)$_2$**	**2-(PMe$_3$)$_2$**	**3**
Chemical Formula	$C_{76}H_{74}AlN_2NiO_2P_3$	$C_{204}H_{199}Al_2N_4Ni_2O_4P_{10}$	$C_{96}H_{130}Al_2N_4Ni_2O_5P_6$	$C_{65}H_{97}AlN_4NiO_4P_3$
Temp	100 K	100 K	100 K	100 K
Crystal system	Monoclinic	Monoclinic	Triclinic	Monoclinic
Space group	$P2_1/c$	$P2_1$	P-1	$P2_1/n$
a/ Å	21.9928(5)	17.4356(2)	13.3950(1)	19.6897(2)
b/ Å	17.5090(4)	48.5980(6)	15.9482(2)	18.2605(2)
c/ Å	17.8697(4)	20.8299(2)	23.2712(3)	40.6637(4)

α/ °	90	90	103.697(1)	90
β/ °	96.555(2)	90.369 (1)	97.850(1)	100.044(1)
γ/ °	90	90	90.485(1)	90
V/ $Å^3$	6836.1(3)	17649.5(3)	4780.4(1)	14396.3(3)
Z	4	4	2	8
D_{calc}/g cm^{-3}	1.191	1.224	1.235	1.086
μ(Mo-Kα) / mm^{-1}	1.548	1.658	2.015	1.469
F(000)	2548	6860	1892	5064
Reflection collected	12180	93407	68604	170067
Independent reflections	9918	54808	39743	47860
R(int)	11.41%	3.90%	3.23%	5.64%
R1 (I > 2σ(I))[a]	6.72%	6.23%	3.78%	7.49%
wR2(all)	18.14%	14.96%	10.03%	16.07%
GOF	1.029	1.071	1.044	1.095

Table S4-2: Primary Coordination Sphere Bond Angles

	1	**2-$(PPh_3)_2$**	***2-$(dppm)_2$**	**2-$(PMe_3)_2$**	**3**
P(1)-Ni-P(2)	117.75(2) °	111.27(5) °	112.94(8) ° 112.49(9) ° 112.39(9) ° 112.65(9) °	107.48(3) ° 112.19(2) °	109.75(4) ° 109.03(4) °
P(1)-Ni-P(3)	-	107.84(5) °	110.51(8) ° 110.48(9) ° 110.67(9) ° 110.03(9) °	113.83(2) ° 109.51(2) °	109.59(4) ° 110.45(4) °
P(2)-Ni-P(3)	-	113.68(6) °	112.84(8) ° 112.35(9) ° 113.12(9) ° 113.08(9) °	113.70(3) ° 113.40(2) °	114.27(4) ° 114.11(4) °
H-Ni-P(1)	112.5(10) ° 115.4(10) °	115.1(15) °	115(5) ° 120(5) °	120.9(10) ° 119.8(12) °	129.4(14) ° 124.0(14) °
H-Ni-P(2)	95.2(10) ° 113.4(10) °	105.9(15)	105(5) ° 102(5) °	101.0(10) ° 102.2(12) °	96.9(15) ° 100.0(14) °
H-Ni-P(3)	-	102.2(17) °	99(5) ° 98(5) °	99.2(10) ° 99.1(12) °	96.3(13) ° 98.9(15) °
Al-H-Ni	94.781° 97.327°	95.679°	90.651° 99.269°	86.142° 85.082°	96.480° 98.423°
N(1)-Al-N(2)	100.77(8) ° 100.74(8) °	109.90(17) °	109.0(3) ° 108.9(3) ° 108.8(3) ° 108.6(3) °	107.94(9) ° 110.16(8) °	107.52(12) ° 107.30(12) °
N(1)-Al-O(1)	77.82(7) ° 76.14(8) °	83.73(16) °	83.8(3) ° 83.9(3) ° 83.0(3) ° 83.3(3) °	82.59(7) ° 82.39(7) °	87.92(12) ° 88.08(12) °
N(2)-Al-O(1)	103.75(8) ° 100.66(8) °	99.62(16) °	103.3(3) ° 101.5(3) ° 102.3(3) ° 102.6(3) °	102.09(8) ° 100.66(7) °	103.78(12) ° 103.30(12) °

N(1)-Al-O(2)	155.91(8) ° 157.76(8) °	-	-	-	-
N(2)-Al-O(2)	79.78(8) ° 77.59(7) °	-	-	-	-
O(1)-Al-O(2)	79.66(8) ° 78.89(7) °	-	-	-	-
H-Al-N(1)	106.6(10) ° 108.1(10) °	128.7(16) °	131(5) ° 135(4) °	138.0(9) ° 136.7(12) °	126.7(9) ° 129.2(11) °
H-Al-N(2)	143.2(10) ° 143.1(10) °	120.7(16) °	118(5) ° 115(4) °	113.9(9) ° 113.1(12) °	116.3(9) ° 115.8(11) °
H-Al-O(1)	105.0(10) ° 107.4(10) °	95.4(15) °	96(5) ° 97(4) °	92.5(9) ° 92.7(12)	108.4(9) ° 106.0(11) °
H-Al-O(2)	86.9(10) ° 84.7(10) °	-	-	-	-

* Hydrides were located in only 2 of 4 of the molecules in the asymmetric unit.

S5: IR Spectroscopy

Figure S5-1: FT-IR spectrum of **1**

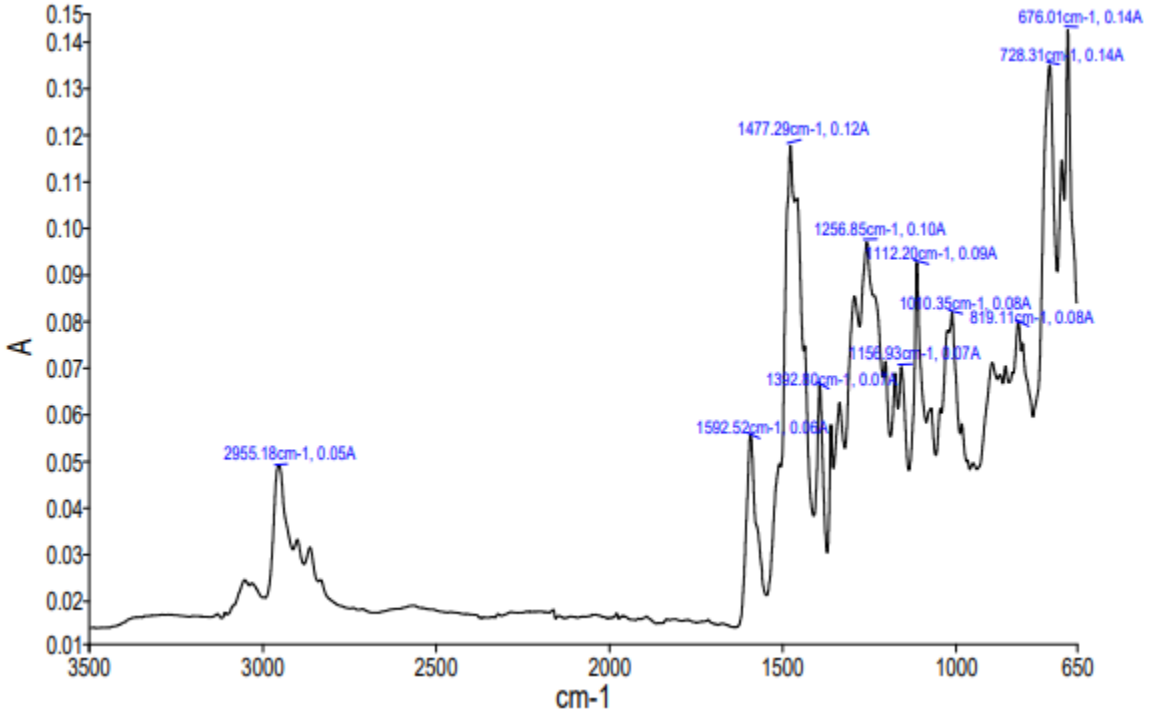

Figure S5-2: FT-IR spectrum of **2-(PPh$_3$)$_2$**

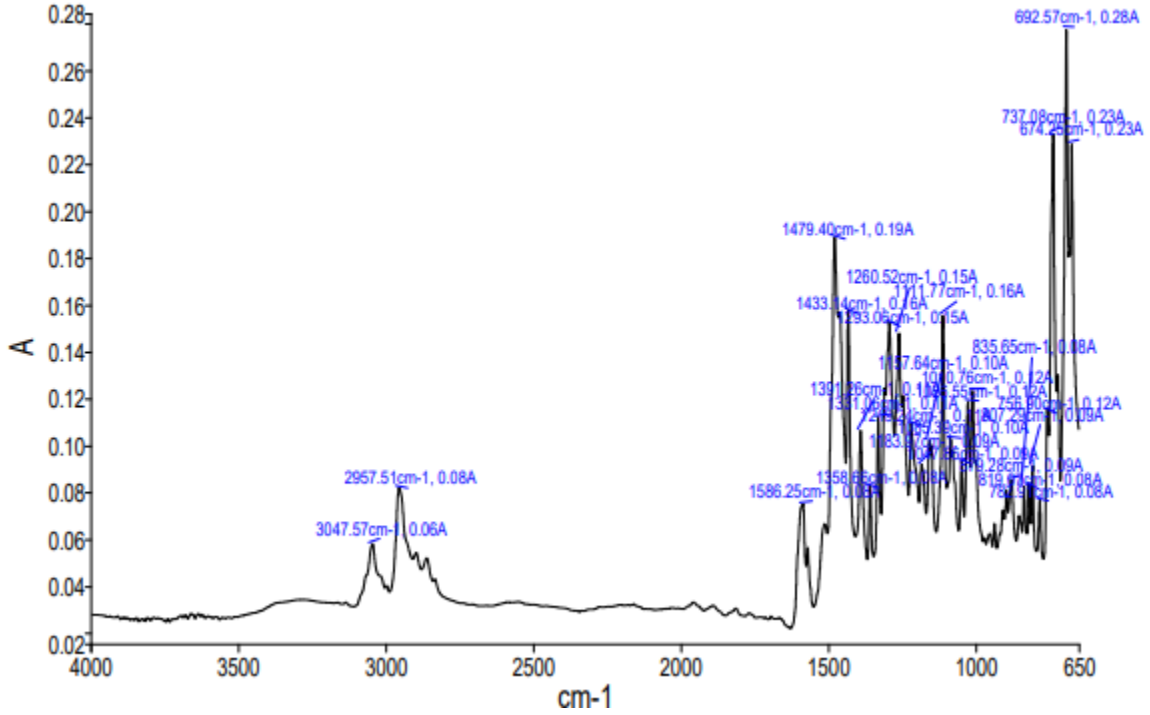

Figure S5-3: FT-IR spectrum of **2-(dppm)$_2$**

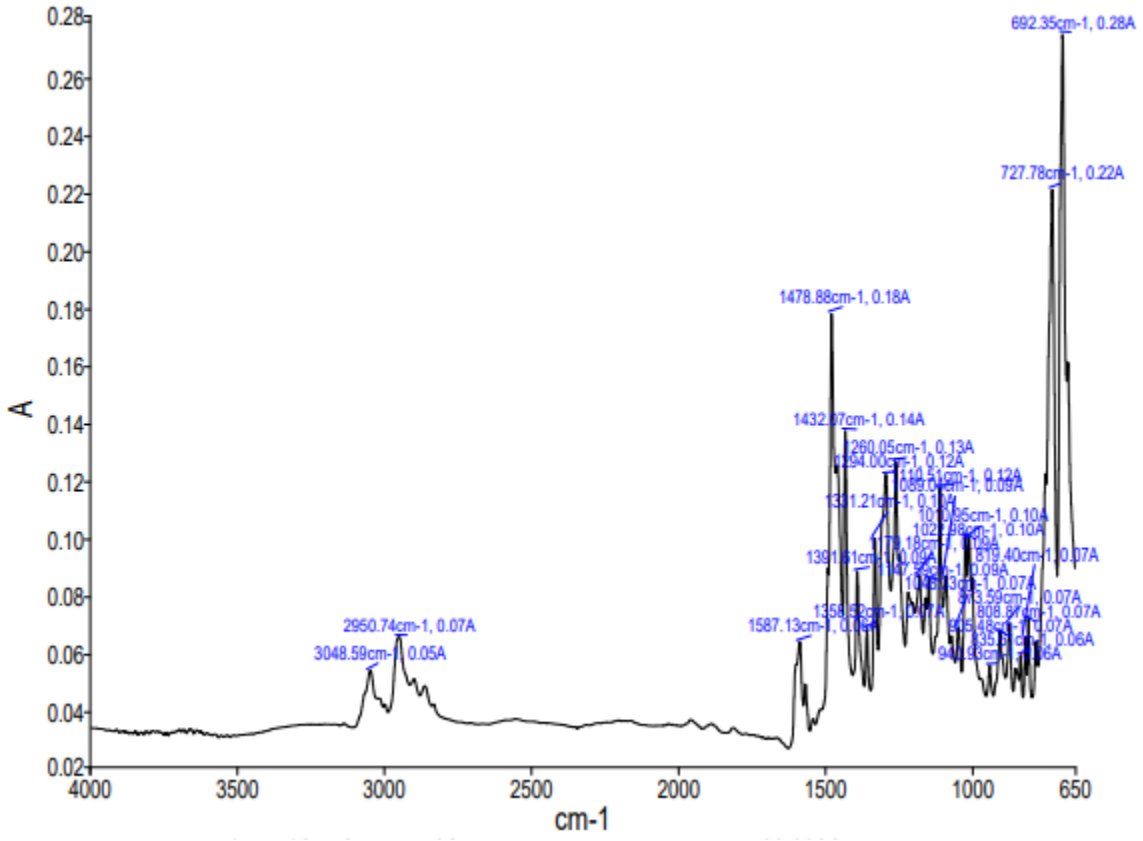

Figure S5-4: FT-IR spectrum of **2-(PMe$_3$)$_2$**

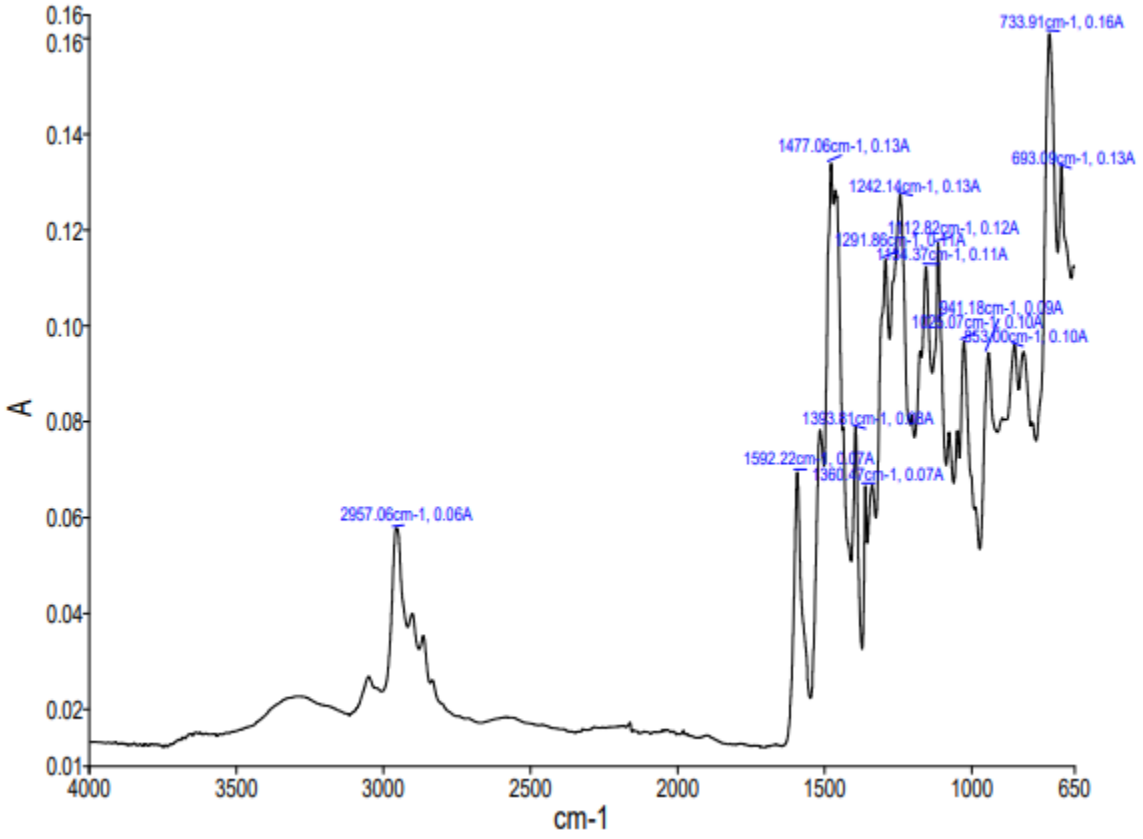

Figure S5-5: FT-IR spectrum of **3**

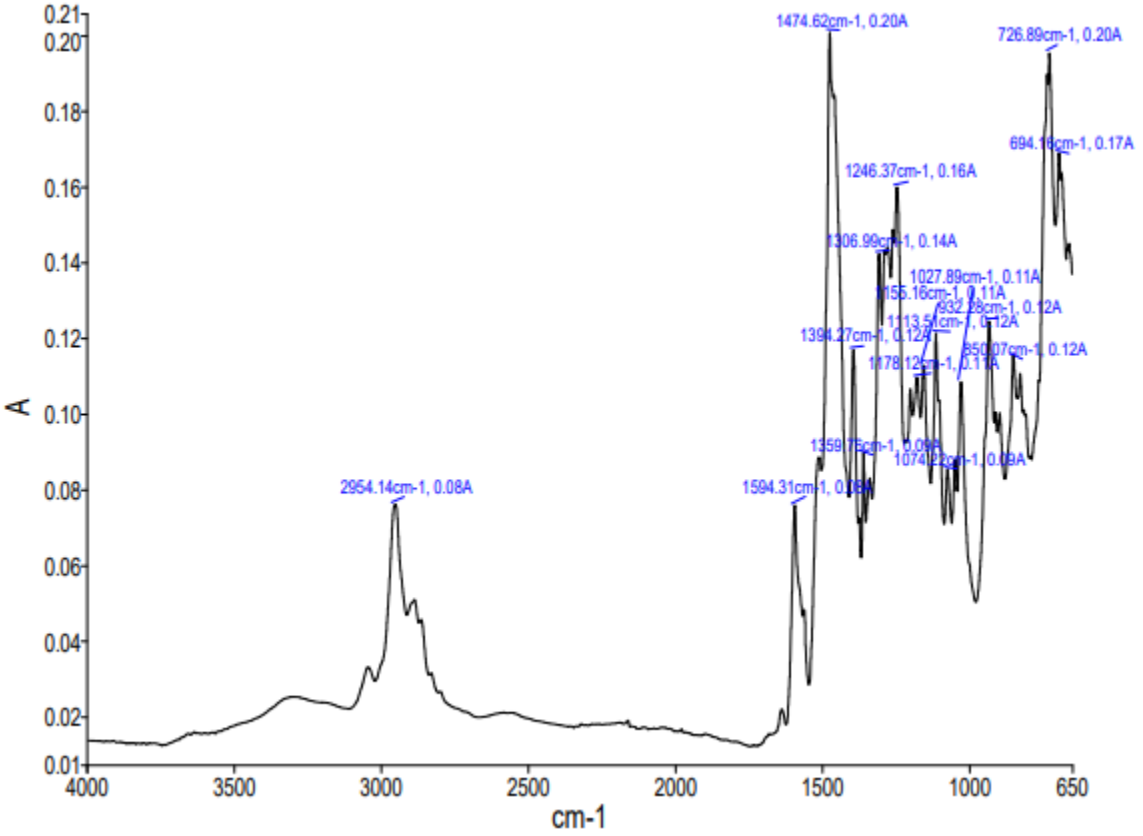

Table S5-1: DFT Calculated IR Stretches for Metal-Hydrides

Complex	νM-H (cm^{-1})
1	1478, 1508
2-$(PPh_3)_2$	1489, 1491
2-$(dppm)_2$	1455, 1457
2-$(PMe_3)_2$	1432
3	1461, 1469, 1475, 1483

References

1) CrysAlisPro 1.171.40.63a (Rigaku Oxford Diffraction, 2019)
2) [SCALE3 ABSPACK -An Oxford Diffraction program(1.0.4,gui:1.0.3) (C) 2005 Oxford Diffraction Ltd.
3) G. M. Sheldrick, Acta Cryst. 2015, A71, 3.
4) O. V. Dolomanov, L. J. Bourhis, R. J. Gildea, J. A. K. Howard, H. Puschmann, J. Appl. Cryst. 2009, 42, 339.
5) G. M. Sheldrick, Acta Cryst. 2008, A64, 112